









# Extracellular Vesicles Regulate Biofilm Formation and Yeast-to-Hypha Differentiation in *Candida albicans*

 Leandro Honorato,<sup>a</sup> Joana Feital Demetrio de Araujo,<sup>a</sup> Cameron C. Ellis,<sup>b</sup> Alicia Corbellini Piffer,<sup>a</sup> Yan Pereira,<sup>a</sup> Susana Frases,<sup>c</sup> Glauber Ribeiro de Sousa Araújo,<sup>c</sup> Bruno Pontes,<sup>d</sup> Maria Tays Mendes,<sup>b\*</sup> Marcos Dias Pereira,<sup>e</sup> Allan J. Guimarães,<sup>f</sup> Natalia Martins da Silva,<sup>a</sup> Gabriele Vargas,<sup>a</sup> Luna Joffe,<sup>g</sup>  Maurizio Del Poeta,<sup>g,h,i</sup> Joshua D. Nosanchuk,<sup>j,k</sup>  Daniel Zamith-Miranda,<sup>j,k</sup> Flávia Coelho Garcia dos Reis,<sup>l,m</sup> Haroldo Cesar de Oliveira,<sup>l</sup> Marcio L. Rodrigues,<sup>l,n</sup> Sharon de Toledo Martins,<sup>l</sup>  Lysangela Ronalte Alves,<sup>l</sup>  Igor C. Almeida,<sup>b</sup>  Leonardo Nimrichter<sup>a</sup>

<sup>a</sup>Laboratório de Glicobiologia de Eucariotos, Departamento de Microbiologia Geral, Instituto de Microbiologia, Universidade Federal do Rio de Janeiro, Rio de Janeiro, Brazil

<sup>b</sup>Department of Biological Sciences, Border Biomedical Research Center, University of Texas at El Paso, El Paso, Texas, USA

<sup>c</sup>Laboratório de Ultraestrutura Celular Hertha Meyer, Instituto de Biofísica Carlos Chagas Filhos (IBCCF), Universidade Federal do Rio de Janeiro, Rio de Janeiro, Brazil

<sup>d</sup>LPO-COPEA, Instituto de Ciências Biomédicas & Centro Nacional de Biologia Estrutural e Bioimagem (CENABIO), Universidade Federal do Rio de Janeiro, Rio de Janeiro, Brazil

<sup>e</sup>Laboratório de Citotoxicidade e Genotoxicidade, Departamento de Bioquímica, Instituto de Química, Universidade Federal do Rio de Janeiro, Rio de Janeiro, Brazil

<sup>f</sup>Laboratório de Bioquímica e Imunologia das Micoses, Departamento de Microbiologia e Parasitologia, Instituto Biomédico, Universidade Federal Fluminense, Niterói, Brazil

<sup>g</sup>Department of Microbiology and Immunology, Stony Brook University, Stony Brook, New York, USA

<sup>h</sup>Department of Microbiology and Immunology and Division of Infectious Diseases, Stony Brook University, Stony Brook, New York, USA

<sup>i</sup>Veterans Affairs Medical Center, Northport, New York, USA

<sup>j</sup>Department of Microbiology and Immunology, Albert Einstein College of Medicine, Bronx, New York, USA

<sup>k</sup>Division of Infectious Diseases, Department of Medicine, Albert Einstein College of Medicine, Bronx, New York, USA

<sup>l</sup>Instituto Carlos Chagas (ICC), Fundação Oswaldo Cruz (FIOCRUZ), Curitiba, Brazil

<sup>m</sup>Centro de Desenvolvimento Tecnológico em Saúde (CDTS), Fundação Oswaldo Cruz, Rio de Janeiro, Brazil

<sup>n</sup>Instituto de Microbiologia Paulo de Góes, Universidade Federal do Rio de Janeiro, Rio de Janeiro, Brazil

Leandro Honorato and Joana Feital Demetrio de Araujo contributed equally to this work. Author order was determined in agreement between both Co-first authors.

**ABSTRACT** In this study, we investigated the influence of fungal extracellular vesicles (EVs) during biofilm formation and morphogenesis in *Candida albicans*. Using crystal violet staining and scanning electron microscopy (SEM), we demonstrated that *C. albicans* EVs inhibited biofilm formation *in vitro*. By time-lapse microscopy and SEM, we showed that *C. albicans* EV treatment stopped filamentation and promoted pseudohyphae formation with multiple budding sites. The ability of *C. albicans* EVs to regulate dimorphism was further compared to EVs isolated from different *C. albicans* strains, *Saccharomyces cerevisiae*, and *Histoplasma capsulatum*. *C. albicans* EVs from distinct strains inhibited yeast-to-hyphae differentiation with morphological changes occurring in less than 4 h. EVs from *S. cerevisiae* and *H. capsulatum* modestly reduced morphogenesis, and the effect was evident after 24 h of incubation. The inhibitory activity of *C. albicans* EVs on phase transition was promoted by a combination of lipid compounds, which were identified by gas chromatography-tandem mass spectrometry analysis as sesquiterpenes, diterpenes, and fatty acids. Remarkably, *C. albicans* EVs were also able to reverse filamentation. Finally, *C. albicans* cells treated with *C. albicans* EVs for 24 h lost their capacity to penetrate agar and were avirulent when inoculated into *Galleria mellonella*. Our results indicate that fungal EVs can regulate yeast-to-hypha differentiation, thereby inhibiting biofilm formation and attenuating virulence.

**IMPORTANCE** The ability to undergo morphological changes during adaptation to distinct environments is exploited by *Candida albicans* and has a direct impact on biofilm formation and virulence. Morphogenesis is controlled by a diversity of stimuli, including

**Invited Editor** David R. Andes, University of Wisconsin—Madison

**Editor** Bernhard Hube, Leibniz Institute for Natural Product Research and Infection Biology—Hans Knoell Institute Jena (HKI)

**Copyright** © 2022 Honorato et al. This is an open-access article distributed under the terms of the [Creative Commons Attribution 4.0 International license](https://creativecommons.org/licenses/by/4.0/).

Address correspondence to Leonardo Nimrichter, [nimrichter@micro.ufrj.br](mailto:nimrichter@micro.ufrj.br).

\*Present address: Maria Tays Mendes, Department of Microbiology and Immunology, University of Maryland School of Medicine, Baltimore, Maryland, USA.

The authors declare a conflict of interest. Dr. Maurizio Del Poeta, M.D. is a Co-Founder and Chief Scientific Officer (CSO) of MicroRid Technologies Inc.

**Received** 10 February 2022

**Accepted** 9 March 2022

**Published** 14 April 2022

osmotic stress, pH, starvation, presence of serum, and microbial components, among others. Apart from external inducers, *C. albicans* also produces autoregulatory substances. Farnesol and tyrosol are examples of quorum-sensing molecules (QSM) released by *C. albicans* to regulate yeast-to-hypha conversion. Here, we demonstrate that fungal EVs are messengers impacting biofilm formation, morphogenesis, and virulence in *C. albicans*. The major players exported in *C. albicans* EVs included sesquiterpenes, diterpenes, and fatty acids. The understanding of how *C. albicans* cells communicate to regulate physiology and pathogenesis can lead to novel therapeutic tools to combat candidiasis.

**KEYWORDS** biofilm, *Candida albicans*, extracellular vesicles, lipids, yeast-to-hypha inhibition

**C***andida albicans* is a common colonizer of the human skin and mucosa (1–3). However, in circumstances where the epithelial barrier, the immune system, and/or the microbiome are compromised, this species can overgrow and cause diseases that range from superficial to disseminated, life-threatening infections (4–6). The ability of *C. albicans* to colonize host tissues is associated with a combination of virulence factors and fitness attributes (4). Among them, a major strategic feature that facilitates *C. albicans*'s ability to persist in different environments is the capacity to switch morphological stages, which is a tightly regulated process called dimorphism, developed by fungal organisms (7).

Different environmental stimuli can induce dimorphism in *C. albicans*. For instance, yeast-to-hypha differentiation is stimulated by *N*-acetylglucosamine (GlcNAc), neutral pH, serum supplementation at 37°C, 5% CO<sub>2</sub>, low nitrogen and amino acids, and diverse other factors (8–12). Dimorphism in *C. albicans* can also be controlled by quorum sensing (QS), a mechanism of microbial communication (13, 14). Farnesol (FOH), farnesoic acid, and tyrosol are major morphogenesis-related QS molecules (QSMs) produced by *C. albicans* (15–17), although other alcohols derived from amino acids have been also characterized (18). FOH and farnesoic acid prevent yeast-to-hypha differentiation with no effects on growth rates (17–19). Tyrosol stimulates germ tube and hypha formation (15). These QSMs are also able to regulate biofilm formation (20, 21). The ability of free fatty acids to inhibit *C. albicans* filamentation and biofilm formation has also been reported (22–24).

Since the first description of fungal extracellular vesicles (EVs) by Rodrigues et al. in 2007 (25), studies have shown that fungal organisms use these compartments as a mechanism of molecular exportation (26–39). Heterogeneous populations of EVs containing lipids, proteins, polysaccharides, pigments, and nucleic acids cross the cell wall outward, reaching the extracellular environment (25, 28, 31, 33, 38, 40). Their implication during pathological and physiological processes is under investigation by a number of groups (29, 37, 41–43). Recently, Bielska and colleagues have shown that EVs isolated from a virulent strain of *Cryptococcus gattii* are efficiently taken up by macrophages previously infected with a nonvirulent strain of the same species (29). Inside phagocytes, the EVs derived from the virulent strain promoted rapid intracellular fungal growth and transferred virulence characteristics to the nonvirulent strain through a mechanism dependent on intact vesicles. The presence of stable RNA and proteins in the EVs was required (29). EVs also have a critical role during biofilm matrix production and drug resistance in *C. albicans* (44, 45).

In this work, we demonstrate that EVs produced by *C. albicans* cells (*C. albicans* EVs) impacted biofilm formation, yeast-to-hypha differentiation, and virulence. Our results reveal previously unknown roles of fungal EVs that impact the physiology and pathogenesis of *C. albicans*.

## RESULTS

**EVs produced by *C. albicans* inhibit biofilm formation.** We began our studies using two distinct approaches to investigate the influence of fungal EVs during biofilm formation. Initially, *C. albicans* yeasts and EV derived from *C. albicans* strain 90028 were

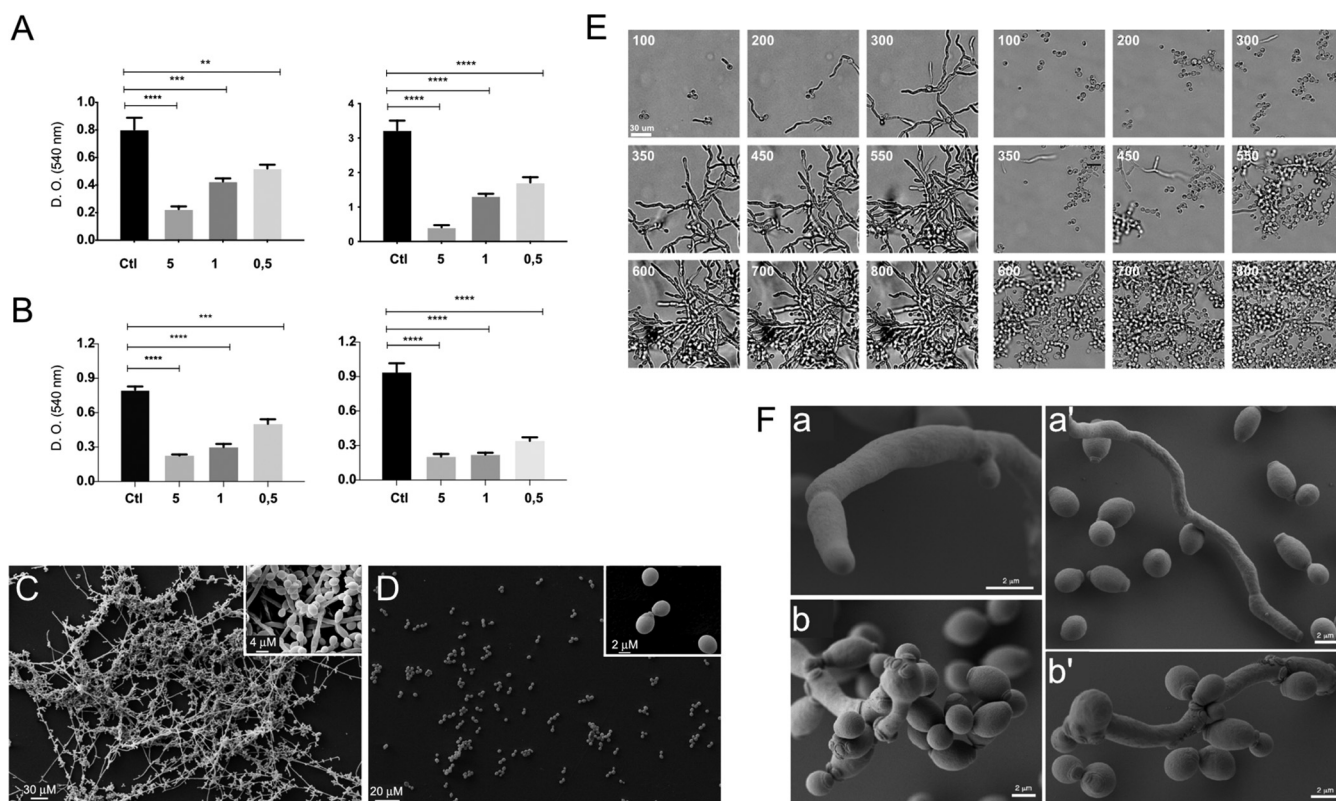


**FIG 1** EVs from *C. albicans* inhibit biofilm formation and yeast-to-hyphae differentiation. Both protocols described in Materials and Methods for EV isolation were used with identical results. The results presented here were obtained from *C. albicans* 90028 EVs (yeast cells) isolated from liquid culture medium. (A) *C. albicans* (90028) ( $10^5$  yeasts) were inoculated into RPMI-MOPS in the presence or absence of *C. albicans* 90028 EVs. Different concentrations of EVs (0.5, 1, and 5  $\mu\text{g/mL}$ , based on sterol content) were added to wells containing *C. albicans* (90028) yeasts, and cells were incubated to develop biofilm for 24 and 48 h in 96-well microplates. (B) *C. albicans* (90028) ( $10^5$  yeasts) were inoculated into RPMI-MOPS and incubated for 90 min. The nonadherent cells were washed out, and fresh medium containing *C. albicans* 90028 EVs (0.5, 1, and 5  $\mu\text{g/mL}$ , based on sterol content) was added. PBS was used as control. Biofilm formation was quantified by crystal violet method. Group comparisons were submitted to one-way analysis of variance (ANOVA) with Dunnett's correction (\*\*,  $P < 0.002$ ; \*\*\*,  $P < 0.001$ ; \*\*\*\*,  $P < 0.0001$ ). (C and D) For SEM, *C. albicans* (strain 90028) yeast cells, untreated (C) or treated with *C. albicans* EVs (5  $\mu\text{g/mL}$ ) (D), were inoculated onto coverslips previously coated with poly-L-lysine in RPMI-MOPS and incubated for 24 h. SEM images show the effect of EVs after 24 h of growth. Insets in panels C and D depict higher magnification of each condition. Bar, 30  $\mu\text{m}$ . (E) *C. albicans* (90028) yeasts were inoculated into M199 medium to induce filamentation in the presence or absence of *C. albicans* 90028 EVs (5  $\mu\text{g/mL}$ , based on sterol content). Cellular density was monitored, and the pictures represent the minutes of incubation (from 100 to 800 min). Bar, 30  $\mu\text{m}$ . Growth under control conditions (absence of *C. albicans* 90028 EVs) and in the presence of *C. albicans* 90028 EVs. The numbers indicate the time in minutes. Bar, 30  $\mu\text{m}$ . (F) *C. albicans* (90028) yeasts were inoculated into M199 medium to induce filamentation in the presence or absence of EVs (5  $\mu\text{g/mL}$ , based on sterol content). SEM of cells after 24 h showing the hyphae and yeasts under control conditions (a and a') in contrast with *C. albicans* 90028 EVs that led to the presence of pseudohyphae with multiple budding sites and yeasts (b and b').

added to wells at the same time. Our results showed that the presence of yeast-derived *C. albicans* EVs negatively impacted biofilm formation in a dose-dependent manner (Fig. 1A). The highest density of EVs (sterol concentration corresponding to 5  $\mu\text{g/mL}$ ) reduced optical density (OD) measurements by approximately 80 to 85% compared to controls with no *C. albicans* EV stimulation. In a second test, to avoid any influence of EVs during the adhesion step, yeasts were added to the wells and incubated for 90 min. Then, the nonadherent cells were removed, and the EVs were added. Similar results were observed, suggesting that the activity of the EVs was independent of the adhesion step (Fig. 1B). SEM images obtained after 24 h of growth (experimental conditions of Fig. 1A) showed that the biofilm formed in the absence of *C. albicans* EVs (control condition) exhibited a standard architecture, with the presence of hyphae, pseudohyphae, and yeast cells attached to the coverslip (Fig. 1C). In contrast with control conditions where the three morphological stages were found, few yeast cells were visualized attached to the coverslip under the condition with EVs present (Fig. 1D). Thus, under the conditions used in our experiments, EVs significantly reduced yeast cell attachment and impaired biofilm formation in *C. albicans*. EV concentrations used in these experiments were initially based on previous studies performed by Bielska and colleagues (29).

**EVs from *C. albicans* inhibit yeast-to-hypha differentiation.** The ability of *C. albicans* 90028 EVs to inhibit biofilm formation suggested that EVs could control morphogenesis in *C. albicans* strain 90028. We then monitored microscopically the impact of *C. albicans* EVs on yeast-to-hypha differentiation induced by M199 medium at 37°C. In the absence of *C. albicans* EVs (control condition), the yeast cells adhered to the solid substrate (Fig. 1E, left) and formed germ tubes after 1 to 2 h of incubation. This step was followed by true hypha formation. Few branching hyphae and yeast cells were visualized after 8 h, but hyphae represented the predominant morphological stage. The time-lapse microscopy of 18 h of incubation is presented as Movie S1 at [10.6084/m9.figshare.19403894](https://doi.org/10.6084/m9.figshare.19403894). In contrast, the addition of EVs drastically changed the phenotype observed (Fig. 1E, right, and Movie S2 at [10.6084/m9.figshare.19403894](https://doi.org/10.6084/m9.figshare.19403894)). Although the yeast cells were attached to the plate and started to form germ tubes, the development of true hypha after elongation was not observed (Fig. 1E, right, and Movie S2 at [10.6084/m9.figshare.19403894](https://doi.org/10.6084/m9.figshare.19403894)). Instead, the appearance of constrictions on elongated cells suggested the development of pseudohyphae after 4 to 7 h. In addition, the cells exposed to *C. albicans* 90028 EVs lost their ability to adhere to the well after 6 h of incubation (Movie S2). Multiple budding points, potentially related to faster growth, were observed along the pseudohyphae, and after 24 h, only yeast cells were detected (Fig. 1E, right, and Fig. 1F). Long pseudohyphae filaments with yeast cells clusters were observed, including a large number of yeast cells derived from pseudohyphae (Fig. 1E, right). Furthermore, there was no indication of cytotoxicity under these conditions since all the yeast cells were able to grow (Movie S2 at [10.6084/m9.figshare.19403894](https://doi.org/10.6084/m9.figshare.19403894)). SEM images show the ultrastructural details of pseudohyphae. Multiple budding yeasts and several bud scars were observed in the experiments with *C. albicans* 90028 EVs added (Fig. 1F). This phenomenon of yeast induction occurred in a dose-dependent manner. A minimum density of *C. albicans* EVs, equivalent to 0.3 to 0.6  $\mu\text{g}$  sterol/mL, was required to inhibit morphogenesis at least partially (Fig. 2A). However, the inhibitory activity was not dependent on the number of yeast cells since different cell suspensions ( $1.5 \times 10^3$  to  $3.5 \times 10^4$  yeast cells/well) were similarly affected using the same density (5  $\mu\text{g}$  sterol/mL) of EVs (data not shown).

Remarkably, a single treatment with EVs was sufficient to impact the yeast-to-hypha differentiation for at least 72 h (Fig. 2B). Aliquots of pretreated yeast cells ( $2.5 \times 10^3$  yeast cells/well) were washed in phosphate-buffered saline (PBS) and plated onto fresh and EV-free M199 medium. The culture was monitored microscopically for 24 h and then transferred again to fresh medium without additional EVs. This process was repeated three times, and aliquots from 48 and 72 h were added to fresh M199 medium for continued microscopic monitoring. Regular hypha formation was observed only after 96 h, 4 days after the initial addition of EVs.

To certify that the inhibitory effect of *C. albicans* 90028 EVs was not due to coisolated contaminants, we fractionated our bioactive samples using size exclusion chromatography (SEC) in a Sepharose CL-4B column. A single peak (fractions 8 to 10) containing proteins and lipids was observed (Fig. S1A and B at [10.6084/m9.figshare.19403894](https://doi.org/10.6084/m9.figshare.19403894)). Dynamic light scattering (DLS) analysis confirmed the presence of EVs in fraction 8 (Fig. S1C at [10.6084/m9.figshare.19403894](https://doi.org/10.6084/m9.figshare.19403894)), corresponding to the most concentrated sample with larger amounts of lipids and proteins, but not in the adjacent ones. Two populations were characterized with average sizes previously reported in our studies (31), ranging from 50 to 120 and 240 to 350 nm, and possibly corresponding to exosomes and ectosomes/microparticles, respectively. The inhibitory activity of the lipids from each fraction was then evaluated. The addition of fraction 8 to yeast cultures inhibited the yeast-to-hypha differentiation of *C. albicans* after 6 h of incubation (Fig. S1D at [10.6084/m9.figshare.19403894](https://doi.org/10.6084/m9.figshare.19403894)). In contrast, fraction 10, where the protein and lipid concentrations were significantly reduced compared to fraction 8, did not modify morphogenesis as efficient hyphae formation occurred. The other fractions in which lipids and proteins were not detected did not inhibit phase transitions (data not shown).

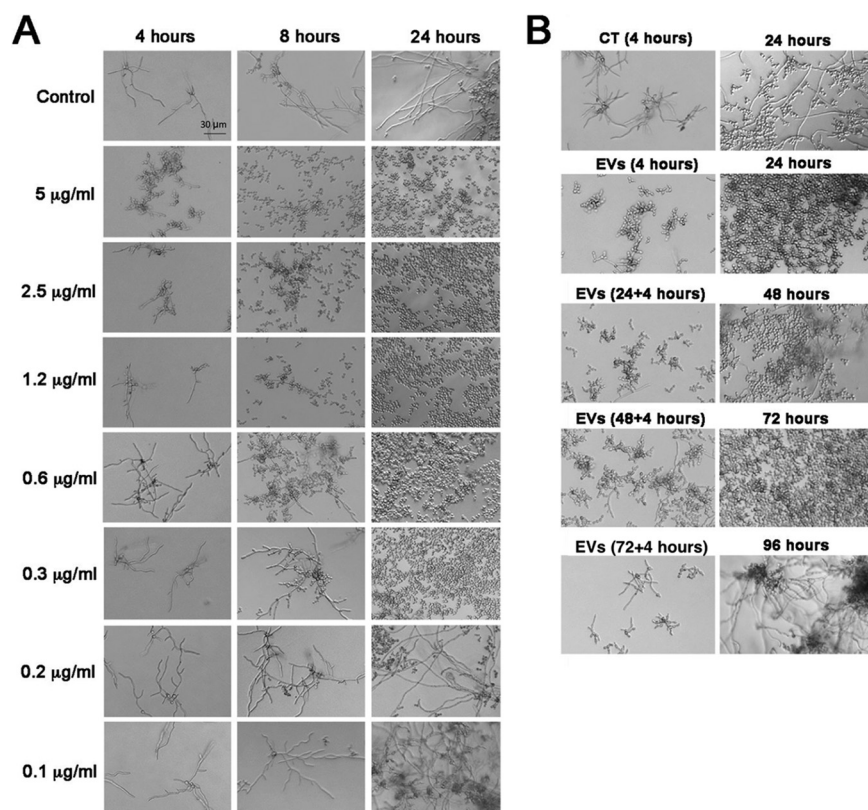


**FIG 2** The inhibitory effect of EVs from *C. albicans* (strain 90028) on yeast-to-hypha conditions is dose dependent and has a long-term effect. (A) *C. albicans* (90028) yeasts were inoculated into M199 (pH 7) in the presence or absence of *C. albicans* 90028 EVs in different concentrations (equivalent to 0.1, 0.2, 0.3, 0.6, 1, 1.2, 2.5, and 5 µg sterol/mL). Bar, 30 µm. (B) The inhibitory effect of a single *C. albicans* EV treatment was tested after 24, 48, 72, and 96 h. Briefly, overnight-treated yeasts were washed with sterile PBS, and aliquots of ( $2.5 \times 10^3$  cells/well) cells were transferred to fresh M199 medium. Yeasts were incubated under the same conditions without addition of EVs for 24 h, and the differentiation was accompanied microscopically. This step was repeated until the reestablishment of *C. albicans* filamentation. Bar, 30 µm. Experiments were performed in biological triplicate with consistent results.

**General properties of EVs produced by different *C. albicans* strains.** EVs produced by different strains of *C. albicans* were isolated from culture supernatants and compared using nanoparticle tracking analysis (NTA) (46). The size distribution of the EVs produced by *C. albicans* strains used in this work ranged from 100 to 500 nm (Fig. 3A to C), similar to measurements published for EVs released by *C. albicans* and other fungal species (31, 46). EVs released by strains SC5314 and 10231 were comparable to each other, ranging from 100 to 400 nm (Fig. 3A and C). EVs produced by strain 90028 were mainly composed of smaller particles, ranging between 100 to 250 nm, but also contained minor populations between 300 and 350 nm and 420 to 480 nm (Fig. 3B). Considering that the *C. albicans* strains released EVs with distinct average size, we normalized our experiments using the total content of sterol in each vesicle preparation, as used in previous studies from our group (31, 34). Of note, this method is highly reproducible and requires small amounts of samples.

**The ability of EVs to inhibit yeast-to-hypha differentiation is reproducible in other strains of *C. albicans*.** We investigated whether the ability to inhibit yeast-to-hypha differentiation was reproducible in EVs obtained from other strains of *C. albicans*. Thus, EVs were isolated from strains with distinct abilities to cause infection. For instance, strain 10231 is less virulent and does not produce FOH (47). Instead, it produces farnesoic acid, an FOH derivative at least 10-fold less active in its ability to inhibit yeast-to-hypha conversion (19). Strains 90028 and SC5314, on the other hand, are regular producers of FOH (17). The results presented in Fig. 3D showed that *C. albicans* EVs from 10231 and SC5314 inhibited hypha formation of strain 90028. However, EVs from these other strains exhibited a reduced effect

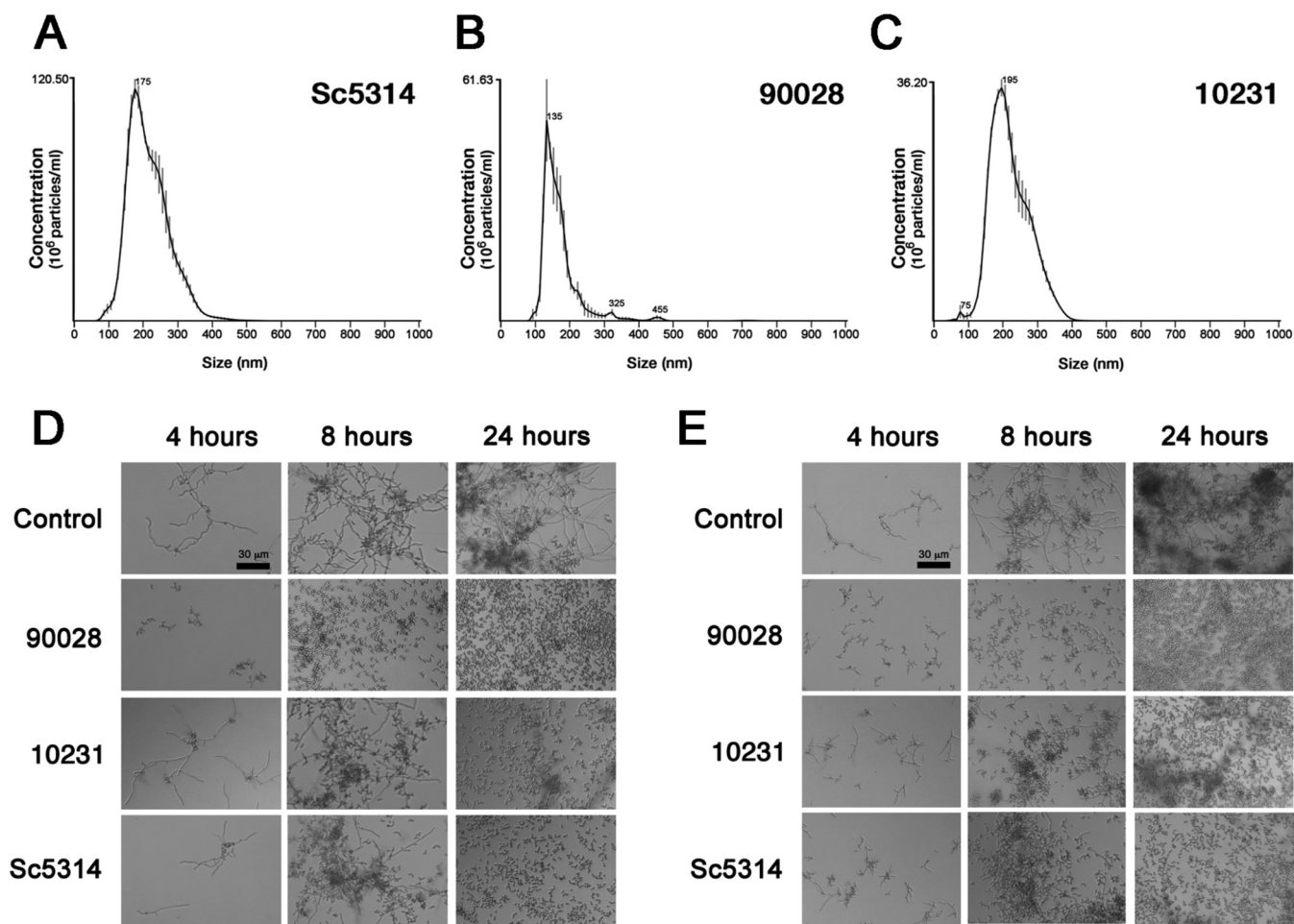


**FIG 3** EVs from different *C. albicans* strains inhibit yeast-to-hyphae transition of strains 90028 and 10231. NTA profile of EVs produced by *C. albicans* strains SC5314 (A), 90028 (B), and 10231 (C) showed similar properties of EVs. *C. albicans* yeast cells of strains 90028 (D) or 10231 (E) were inoculated into M199 (pH 7) in the presence or absence of *C. albicans* EVs (equivalent to 5 μg sterol/mL) from distinct strains of *C. albicans* (90028, 10231, and SC5314). The effects were visualized after 4, 8, and 24 h. PBS was added alone as a control. Bar, 30 μm. Experiments were performed four times with consistent results.

at the initial times of incubation compared to *C. albicans* 90028 EVs, indicating that although each strain’s EVs had the ability to inhibit filamentation, they may have a distinct potency. To confirm that the effect was not strain specific, we evaluated the effect of the EVs produced by strains 10231 and 90028 on the morphogenesis of strain 10231 (Fig. 3E). The EV-mediated inhibition of filamentation of strain 10231 was confirmed. The recovery of EVs was similar using solid or liquid medium (average of 0.16 and 0.18 μg of sterol/10<sup>9</sup> cells, respectively). Further experiments were performed using EVs produced by the 90028 strain cultivated in liquid medium since this condition resulted in better yields of EVs.

**EV molecules with yeast-to-hypha inhibitory activity are thermoresistant and enriched in preparations containing nonpolar lipids.** The ability to prevent yeast-to-hypha differentiation was preserved by *C. albicans* 90028 EVs after heating them at 90°C for 15 min (Fig. 4A), suggesting that thermoresistant molecules could be mediating the inhibitory effect. Since lipids participate in *C. albicans* morphogenesis (16, 21), we extracted and fractionated the lipid components contained in *C. albicans* 90028 EVs and tested their inhibitory activity. The crude lipid extract was partitioned using standardized protocols to enrich lipids according to their polarity (48), and the organic (lower and upper) phases were added to yeast suspensions in M199 medium for microscopic monitoring of morphogenesis. The lower phase (LP) activity was very similar to *C. albicans* 90028 EVs in its ability to inhibit differentiation (Fig. 4B). Although the upper phase (UP) was also active, its effect was observed only after 24 h of incubation. The precipitate

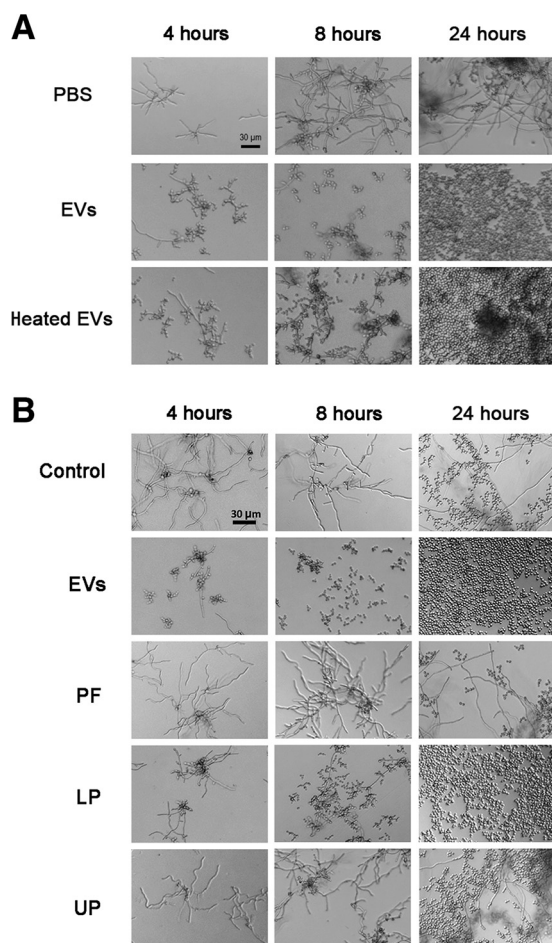


**FIG 4** Thermoresistant molecules carried by *C. albicans* EVs are associated with yeast-to-hyphae inhibitory effect. (A) *C. albicans* (90028) yeast cells were inoculated into M199 (pH 7) in the presence or absence of *C. albicans* 90028 EVs or heat-treated EVs in a concentration equivalent to 5 μg sterol/mL. The effect was visualized after 4, 8, and 24 h. PBS was added alone as a control. Bar, 30 μm. The results shown are representative of three independent experiments. (B) *C. albicans* (90028) yeasts were inoculated into M199 in the presence or absence of *C. albicans* EVs, EV-derived protein-rich fraction (PF), or lipid lower (LP) or upper phase (UP) in a concentration equivalent to 5 μg sterol/mL. The effect was visualized after 4, 8, and 24 h. PBS was added alone as a control. Bar, 30 μm.

(protein-rich fraction [PF]) obtained from *C. albicans* 90028 EV lipid extraction, likely rich in proteins, had no apparent influence on morphogenesis (Fig. 4B). The LP of lipids extracted from the whole cells were also able to inhibit *C. albicans* differentiation (data not shown). LP obtained from liquid Sabouraud (no yeast cells, control medium) using the same extraction and partition protocol showed no activity (data not shown).

**EVs produced by other fungal species affect yeast-to-hypha differentiation in *C. albicans*.** Based on the lipid nature of the bioactive molecules studied in our work and the fact that FOH and farnesoic acid are QSM lipids that control yeast-to-hypha differentiation in *C. albicans* (16, 21, 23), we hypothesized that the presence of FOH and farnesoic acid in EVs from *C. albicans* could result in filamentation inhibition. To confirm this possibility, we asked whether EVs from *S. cerevisiae*, which synthesizes and exports FOH in very small amounts (49), would regulate morphogenesis in *C. albicans*. We also included EVs from *H. capsulatum* in these analyses since FOH or FOH derivatives have not been characterized as lipid components in this fungus. We first investigated whether the strains used in our study produced detectable amounts of FOH into the LP by reverse-phase thin-layer chromatography (TLC). Whole cells were used in order to obtain larger amounts of lipids. The TLC showed a sharp band in the LP of *C. albicans* (strain 90028) with identical color and retention factor ( $R_f$ ) obtained for an

FOH standard, strongly indicating the presence of this molecule in the *C. albicans* extract (Fig. S2A at [10.6084/m9.figshare.19403894](https://doi.org/10.6084/m9.figshare.19403894)). A band with a similar  $R_f$  was observed in the LP of *H. capsulatum*; however, a distinct yellowish color was visualized (Fig. S2A). Thus, a more detailed structural analysis was necessary to confirm the chemical nature of that band, as further described in this section. No molecules migrating as FOH were detected in the LP from *S. cerevisiae*. Nevertheless, EVs from these three species were able to impair *C. albicans* hypha formation (Fig. S2B at [10.6084/m9.figshare.19403894](https://doi.org/10.6084/m9.figshare.19403894)). Clearly, the kinetics of inhibition (comparing 8 h versus 24 h of incubation time) observed for EVs released by *H. capsulatum* and *S. cerevisiae*, as well as for *C. albicans* 10231 EVs, were considerably slower than *C. albicans* 90028 EVs. With *H. capsulatum* EVs, the inhibitory effect was observed only after an overnight incubation. The first signals of inhibitory effect from *S. cerevisiae* EVs were detected after 8 h of incubation, an effect comparable with EVs from *C. albicans* strain 10231 (Fig. 3D). To confirm that the inhibitory effect was not pleiotropic, caused by EVs produced by any of the organisms studied, we also tested the activity of EVs from murine macrophages-like (MOs). Contrasting with the activity of fungal EVs, MO EVs did not interfere with yeast-to-hypha differentiation *in vitro* (Fig. S2B at [10.6084/m9.figshare.19403894](https://doi.org/10.6084/m9.figshare.19403894)). The fact that EVs lacking or expressing reduced levels of FOH inhibit *C. albicans* differentiation, even at a lower efficacy, suggests that other EV molecules, in addition to FOH, also participate in the inhibitory mechanisms. We next investigated whether other lipids could be potentially involved in the inhibitory effect of EVs.

**Terpenes and fatty acids are the major compounds potentially involved with *C. albicans* yeast-to-hypha inhibition.** To investigate whether other lipids produced by *C. albicans* 90028 could mediate the inhibitory activity of *C. albicans* EVs, we tested the distinct TLC bands from the *C. albicans* LP extract. Using a preparative TLC plate and staining the lipids with mild iodine vapor, to avoid lipid degradation, we obtained five major fractions (A to E) corresponding to separate bands (Fig. S3 at [10.6084/m9.figshare.19403894](https://doi.org/10.6084/m9.figshare.19403894)). The ability of each fraction to inhibit yeast-to-hypha differentiation was investigated, and only one (band A), with an  $R_f$  similar to an authentic FOH standard, showed an active effect (Fig. S3).

We then concentrated our efforts on the analysis of FOH in fungal EVs and lipid extracts. To that end, we followed a protocol previously used for FOH extraction and employed a highly sensitive gas chromatography-mass spectrometry with selected reaction monitoring (GC-MS/SRM) method, using an external bona fide standard of FOH (50, 51). As observed in Fig. 5A and B (black line), the FOH standard (at 4.5 pmol/ $\mu$ L, 1  $\mu$ L injection) is comprised of a mixture of four isomers (2-*cis*,6-*cis*-farnesol [Z,Z-FOH], 2-*cis*,6-*trans*-farnesol [Z,E-FOH], 2-*trans*,6-*cis*-farnesol [E,Z-FOH], and 2-*trans*,6-*trans*-farnesol [E,E-FOH]), which clearly separated from each other using the GC gradient conditions employed. The isomer profile was comparable to that previously reported (51). Under the experimental conditions used for the standard mixture, we detected peaks (at 9.65 and 9.81 min) with SRM transitions (not shown) and full-scan chromatogram elution times similar to Z,E-FOH and E,E-FOH isomers (peaks 3 and 5, respectively) in the *C. albicans* 90028 yeast EV sample (Fig. 5A and B). Table 1 shows the relative peak intensity of these FOH isomers and other identified compounds found in fungal EVs and other lipid fractions. Besides the two FOH isomers, the GC-MS analysis revealed that *C. albicans* 90028 EVs contained large amounts of other terpenoids or isoprenoids such as geranylgeraniol isomers and, to a much lesser extent, squalene (Table 1).

Using the standard calibration curve from the d6-E,E-FOH isomer, we quantified the amounts of each isoprenoid/terpenoid found in the fungal EVs (Table 2), confirming the results above and showing a significant enrichment of isoprenoids in EVs carried by *C. albicans* strain 90028. The FOH derivative 2,3-dihydro-6-*trans*-farnesol (6, 10-dodecadienol-1-ol, 3,7,11 trimethyl) (peak 1) and related isoprenoid, 2,3-dihydro-6-*trans*-geraniol (6,10,14-hexadecatrien-1-ol, 3,7,11,15 tetramethyl) (peak 9), corresponding to FOH and geranylgeraniol units lacking a double bond at C-2, respectively, were also characterized as major peaks (Fig. 5; Tables 1 and 2). The lipid content of *C. albicans* 10231 LP and EVs



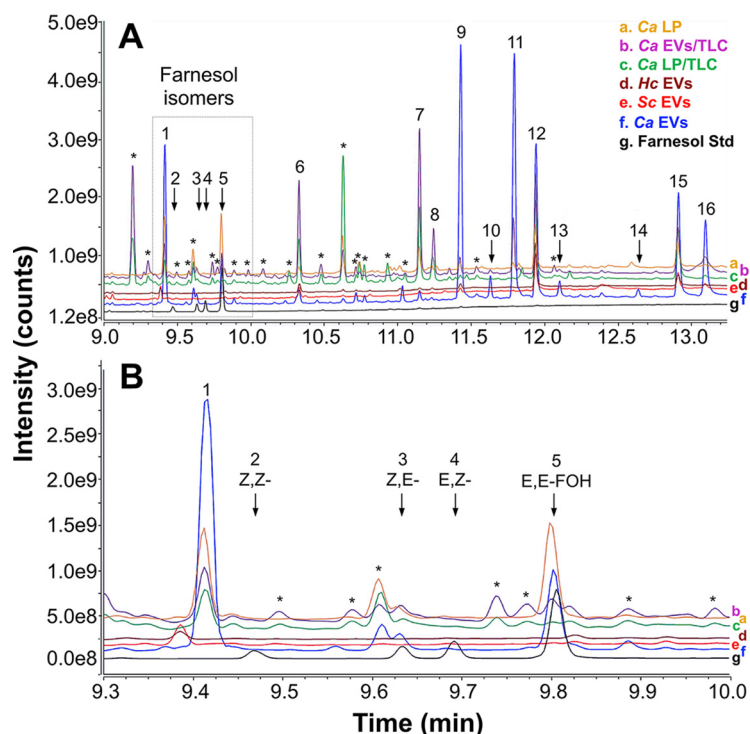


**FIG 5** GC-MS analysis of fungal lipids and EVs. Lipids were extracted from the *C. albicans* 90028 LP fraction and EVs and from the RP-TLC band comigrating with farnesol in the two samples. Lipids were also extracted from *H. capsulatum* and *S. cerevisiae* EVs. The resulting samples were analyzed by GC-MS/MS. (A) GC-MS full-scan chromatogram. (B) The chromatogram region containing the four farnesol isomers is indicated (dashed rectangle) and shown in detail. A standard mixture containing the four farnesol isomers (Z,Z-, Z,E-, E,Z-, and E,E-FOH) was used as reference (black line/trace). The GC-MS full-scan traces were overlaid and labeled (a to g) to facilitate visualization and comparison. Farnesol isomers and peaks of interest are indicated numerically and annotated in Table 1. Asterisks indicate contaminants (e.g., phthalates and other plasticizers) or compounds not identified in the library (low structural match probability). Ca, *C. albicans*; Hc, *H. capsulatum*; Sc, *S. cerevisiae*.

was also analyzed (Fig. S4 at [10.6084/m9.figshare.19403894](https://doi.org/10.6084/m9.figshare.19403894)). In the experimental conditions used, we could not detect any FOH or DHFOH isomers in the *C. albicans* 10231 LP and EVs, suggesting that the ability to produce FOH in this strain is completely abrogated (Fig. S4; Fig. 5; Tables 1 and 2). The peak observed at 9.58 min by GC-MS analysis, with similar retention time as Z,E-FOH, was identified as a contaminant in the NIST mass spectral library (Fig. S4 and Table S1 at [10.6084/m9.figshare.19403894](https://doi.org/10.6084/m9.figshare.19403894)). Of those isoprenoids, only 2,3-dihydro-6-*trans*-geraniol was also found in *H. capsulatum* and *S. cerevisiae* EVs. None of the FOH isomers or its derivative (2,3-dihydro-6-*trans*-farnesol [dihydrofarnesol or DHFOH]) were detected in the EVs from *H. capsulatum* and *S. cerevisiae*, confirming that these molecules are only enriched in *C. albicans* 90028 EVs (Fig. 5; Tables 1 and 2). Together, these data confirm that although the terpenes considerably increased the inhibitory activity of *C. albicans* 90028 EVs, they are not the only lipids able to control *C. albicans* filamentation.

The other class of lipids recognized to inhibit hyphal growth and biofilm formation in *C. albicans* is the fatty acids (22, 23, 52). In our analysis, five fatty acids were identified as major *C. albicans* 90028 EV components, including octadecanoic (stearic acid, C<sub>18:0</sub>) and octadecenoic (oleic acid, C<sub>18:1</sub>) acids, and, to a much lesser extent, (9Z)-hexadec-9-enoic (palmitoleic acid, C<sub>16:1</sub>), dodecanoic (lauric acid, C<sub>12:0</sub>), and tetradecanoic (myristic acid, C<sub>14:0</sub>) acids (Fig. 5 and Table 1). Remarkably, larger amounts of myristic and stearic acid were found enriched in *C. albicans* 10231 EVs, along with small amounts of pentadecyloic acid, C<sub>16:1</sub> and C<sub>18:1</sub> (Fig. S4). Fatty acids were also found in EVs from *H. capsulatum* (C<sub>12:0</sub>, C<sub>14:0</sub>, and C<sub>18:0</sub>) and *S. cerevisiae* (C<sub>12:0</sub>, C<sub>14:0</sub>, C<sub>16:1</sub>, C<sub>18:0</sub>, and C<sub>18:1</sub>) (Fig. 5 and Table 1). Large amounts of ascorbic acid 2,6-dihexadecanoate were

**TABLE 1** Major lipid compounds identified by GC-MS/MS in the lipid LP fractions and EVs of *C. albicans* and EVs of *H. capsulatum* and *S. cerevisiae*

Peak no.	RT (min)	Compound	Peak relative intensity (%) of fungal preparation/fraction:					
			<i>C. albicans</i>				<i>H. capsulatum</i>	<i>S. cerevisiae</i>
			LP	EVs	LP/TLC	EVs/TLC	EVs	EVs
1	9.42	2,3-Dihydro-6- <i>trans</i> -farnesol (6,10-dodecadien-1-ol, 3,7,11 trimethyl)	93	63	32	25	ND <sup>a</sup>	ND
2	9.47	2,6- <i>Cis</i> -farnesol (Z,Z-farnesol)	ND	ND	ND	ND	ND	ND
3	9.63	2- <i>Cis</i> ,6- <i>trans</i> -farnesol (Z,E-farnesol)	ND	4	ND	7	ND	ND
4	9.68	2- <i>Trans</i> ,6- <i>cis</i> -farnesol (E,Z-farnesol)	ND	ND	ND	ND	ND	ND
5	9.81	2,6- <i>Trans</i> -farnesol (E,E-farnesol)	100	20	5	9	ND	ND
6	10.33	Dodecanoic acid (lauric acid, C <sub>12:0</sub> )	14	5	57	67	25	23
7	11.15	Tetradecanoic acid (myristic acid, C <sub>14:0</sub> )	41	4	97	100	6	4
8	11.25	Dodecanoic acid, undecyl ester (C <sub>23:0</sub> -O <sub>2</sub> )	ND	ND	30	32	6	4
9	11.42	2,3-Dihydro-6- <i>trans</i> -geraniol (6,10,14-hexadecatrien-1-ol 3,7,11,15 tetramethyl)	14	100	8	12	19	9
10	11.63	Geranylgeraniol (isomer 1) <sup>b</sup>	ND	9	ND	3	ND	ND
11	11.79	Geranylgeraniol (isomer 2) <sup>b</sup>	10	97	ND	39	ND	ND
12	11.93	Ascorbic acid 2,6-dihexadecanoate	72	60	100	68	100	100
13	12.11	(9Z)-hexadec-9-enoic acid (palmitoleic acid, C <sub>16:2</sub> )	ND	7	3	3	ND	4
14	12.64	Squalene	ND	3	ND	ND	ND	ND
15	12.92	Octadecanoic acid (stearic acid, C <sub>18:0</sub> )	41	41	62	30	38	36
16	13.12	Octadecenoic acid (oleic acid, C <sub>18:1</sub> )	3	30	5	10	ND	14

<sup>a</sup>ND, not detected (below the method's limit of detection).

<sup>b</sup>We were unable to determine the precise structures of these geranylgeraniol geometric isomers through fragmentation spectral library matching.

found in EVs from all species except for the *C. albicans* strain 10231 (Fig. 5, Fig. S4, Table 1, and Table S1).

We also characterized the major lipids found in the LP from *C. albicans* and its bioactive TLC-derived band (Fig. S3). Equivalent amounts of DHFOH and E,E-FOH were detected in *C. albicans* 90028 LP (Table 1). The derivative 2,3-dihydro-6-*trans*-geraniol was also identified in *C. albicans* 90028 LP (Tables 1 and 2). Moreover, the free fatty acids C<sub>12:0</sub>, C<sub>14:0</sub>, C<sub>18:0</sub>, and C<sub>18:1</sub> were also characterized in this fraction. Finally, we resolved the lipids from *C. albicans* 90028 EVs by RP-TLC, and the band corresponding to the FOH R<sub>f</sub> was also analyzed. We found a high similarity between the total EV lipids and this band, with a clear enrichment of FOH isomers and FOH-like structures and other isoprenoids/terpenoids (Tables 1 and 2). In addition, we observed an enrichment of the fatty acids C<sub>12:0</sub> and C<sub>14:0</sub>, and dodecanoic acid undecyl ester (C<sub>23:0</sub>-O<sub>2</sub>) (Fig. 5A and Table 1).

**DHFOH and FOH similarly reproduce the effects of *C. albicans* EVs on filamentation.** As mentioned previously, FOH is a major QSM produced by *C. albicans* with the ability to block filamentation (17, 53). Given that the major terpenes carried by EVs from *C. albicans* strain 90028 are DHFOH and 2,3-dihydro-6-*trans*-geraniol (Table 1), we investigated the efficacy of a commercially available, synthetic DHFOH to inhibit *C. albicans* filamentation. First, this standard was analyzed by GC-MS to confirm

**TABLE 2** Quantification of FOH and FOH-like structures in lipid LP fractions and EVs of *C. albicans* and EVs from *H. capsulatum* and *S. cerevisiae*

Fungal fraction/prepn	Farnesol isomers (ng/100 μg total lipid or protein) in compound: <sup>a</sup>			Farnesol-like structures (ng/100 μg total lipid or protein) in compound: <sup>a</sup>		
	2,3-Dihydro-6- <i>trans</i> -farnesol	Z,E-FOH	E,E-FOH	2,3-Dihydro-6- <i>trans</i> -geraniol	Geranylgeraniol (isomer 1)	Geranylgeraniol (isomer 2)
<i>C. albicans</i> LP	16.3	1.8	19	2.1	ND	1.2
<i>C. albicans</i> LP/TLC	2.1	ND <sup>b</sup>	ND	ND	ND	ND
<i>C. albicans</i> EVs	33.7	1.6	9.7	67	4.1	63.4
<i>C. albicans</i> EVs/TLC	48.8	7.5	9.6	21	ND	77.4
<i>H. capsulatum</i> EVs	ND	ND	ND	4.7	ND	1.9
<i>S. cerevisiae</i> EVs	ND	ND	ND	1.2	ND	ND

<sup>a</sup>LP and LP/TLC fractions were normalized by 100 μg of total lipid, whereas all EV preparations were normalized by 100 μg of protein.

<sup>b</sup>ND, not detected (below the method's limit of detection).

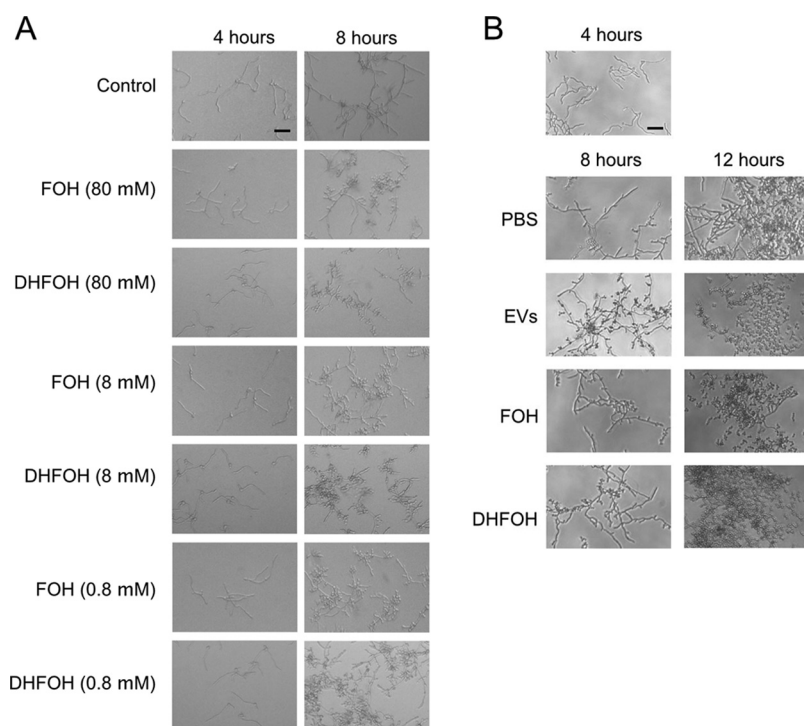


**FIG 6** *C. albicans* EVs, FOH, and DHFOH reversed the yeast-to-hypha differentiation. (A) *C. albicans* (90028) yeast cells were inoculated into M199 (pH 7) in the presence or absence of distinct concentrations of FOH or DHFOH. (B) *C. albicans* (90028) yeasts were inoculated into M199 and incubated for 4 h to induce hyphae formation. Then, PBS (control), *C. albicans* EVs (5  $\mu$ g/mL), FOH (25  $\mu$ M), or DHFOH (25  $\mu$ M) were added to the wells. Cell morphology was visualized after 8 and 12 h. Bars, 30  $\mu$ m.

its purity and integrity (data not shown). The bona fide standard exhibited an activity similar to FOH (Fig. 6A and B). Of note, the biological activities of commercial FOH and DHFOH were considerably reduced within a few weeks in stock solution at  $-20^{\circ}\text{C}$  (data not shown). On the other hand, synthetic geranylgeraniol and ascorbic acid 2,6-dihexadecanoate were not able to interfere with yeast-to-hypha differentiation (data not shown). Unfortunately, 2,3-dihydro-6-*trans*-geraniol, observed in *C. albicans* 90028 LP and EVs (Fig. 5 and Table 1), was not commercially available as synthetic or purified compound, and therefore, its biological activity could not be confirmed.

**EVs from *C. albicans* yeast cells reverse the yeast-to-hypha differentiation.** We next investigated whether *C. albicans* EVs were able to reverse the yeast-to-hypha differentiation induced by M199 medium. Yeast cells were plated onto M199, and hypha formation was observed after 4 h of induction (Fig. 6B), at which time *C. albicans* EVs, FOH, or DHFOH were added to the wells. Yeast cells were visualized 4 h after the addition of *C. albicans* EVs to the filamentous cultures, indicating that fungal EVs and the terpenes were able to efficiently reverse the yeast-to-hypha morphogenesis, even after the highly regulated process had been initiated.

**Inhibitory activity caused by *C. albicans* EVs is reversed by db-cAMP addition.** FOH stops *C. albicans* filamentation by inhibiting adenylate cyclase (Cyr1) (54). This effect is rescued *in vitro* by the addition of exogenous db-cAMP (55). To investigate whether the EVs' inhibitory effect is mediated by Cyr1 repression, we performed two experiments. First, we incubated db-cAMP and *C. albicans* 90028 EVs for 1 h and then added the mixture to *C. albicans* yeasts. Under these experimental conditions, the db-cAMP had no effect, and the inhibitory activity was similar to *C. albicans* EVs alone (Fig. 7). These results indicated that the EVs are not inhibiting Cyr1 and suggested that other signaling mechanisms could be involved. However, we cannot rule out that the EVs sequestered or hydrolyzed the db-cAMP. To address these possibilities, we first treated *C. albicans* yeasts with EVs for 1 h, and then db-cAMP was added to the system. Under these conditions, the filamentation was observed after 8 h, confirming that Cyr1

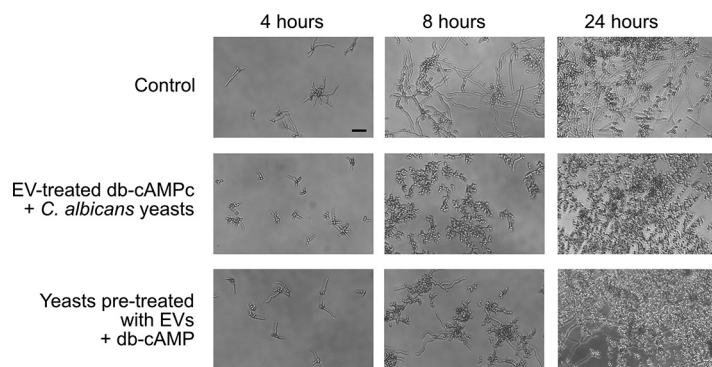


**FIG 7** The reversing effect on *C. albicans* morphogenesis caused by db-cAMP is inactivated by preincubation with *C. albicans* EVs. db-cAMP preincubated with EVs (5  $\mu\text{g}/\text{mL}$ ) does not reverse the inhibitory effect of *C. albicans* 90028 EVs on *C. albicans* phase transition. The addition of db-cAMPc (10 mM) reverses the yeast-to-hyphae inhibition caused by *C. albicans* 90028 pretreated with *C. albicans* 90028 EVs. Bar, 30  $\mu\text{m}$ .

was targeted by *C. albicans* EV activity (Fig. 7). However, after 24 h, we observed that the control conditions (PBS) exhibited a higher proportion of hyphae than the conditions where db-cAMP was added to yeasts pretreated with EVs. These results suggested that although Cyr1 seems to be a major target for *C. albicans* EVs, other mechanisms might also be involved.

**Treatment with EVs reduces the ability of *C. albicans* to penetrate solid medium and decreases fungal virulence in a *Galleria mellonella* model of candidiasis.** Due to the well-established connections between pathogenesis and morphological transitions in *C. albicans* (12), we investigated whether treatment with *C. albicans* EVs could abrogate the ability of the fungus to penetrate solid medium, a consequence of filamentous growth regularly correlated with virulence (56). Colonies of *C. albicans* cultivated in M199 agar medium produced normal hypha at the edges after 5 to 6 days of invasive growth (Fig. 8A, top left panel). In contrast, after 5 to 6 days, no hyphae were visualized when yeast cells were pretreated with *C. albicans* EVs (Fig. 8A, top right panel). In fact, under *C. albicans* EV treatment conditions, hypha formation was only observed after 10 to 11 days of incubation (data not shown). These results were confirmed using the plate-washing method (56). After 10 days of growth, the colonies (control and EV treated) were washed using the same flow rate, water temperature, and duration of time (Fig. 8A, bottom panels), producing results that were similar to those obtained under standard conditions.

The capacity to reduce the adhesive and invasive abilities of *C. albicans* indicated that preincubation of yeast cells with *C. albicans* EVs could decrease the virulence of *C. albicans*. To investigate whether the treatment of yeast cells with EVs would impact pathogenesis, we used *G. mellonella* as a model. Infection of *G. mellonella* larvae with a lethal inoculum of yeast cells of *C. albicans* cultivated in standard medium without *C. albicans* EVs caused melanization and death in 80% of the animals in less than 1 week (Fig. 8B). Remarkably, when the pretreated yeast cells were used to infect the larvae, only 5 to 10% of the animals died (Fig. 8B, experiments 1 and 2). We then evaluated the ability of EVs to impair *C. albicans* differentiation in the presence of serum, a major hyphae-inducing factor in mammalian hosts (57). Our results demonstrated that *C. albicans* EVs were able to inhibit yeast-to-hypha differentiation in the presence of serum and  $\text{CO}_2$  (Fig. 8C). Together, these data suggested that *C. albicans* EVs could directly affect the pathogenesis of *C. albicans* during the infection.

## DISCUSSION

Our results demonstrated that the addition of *C. albicans* 90028 EVs strongly inhibited biofilm development of *C. albicans*. In addition, their filamenting-suppressing activity was similar to the effect of FOH. The effect was notably prolonged, indicating that yeast-to-hyphae morphogenesis was temporarily turned off. The exact mechanism and signaling pathways triggered by *C. albicans* EVs that promoted the long-lasting

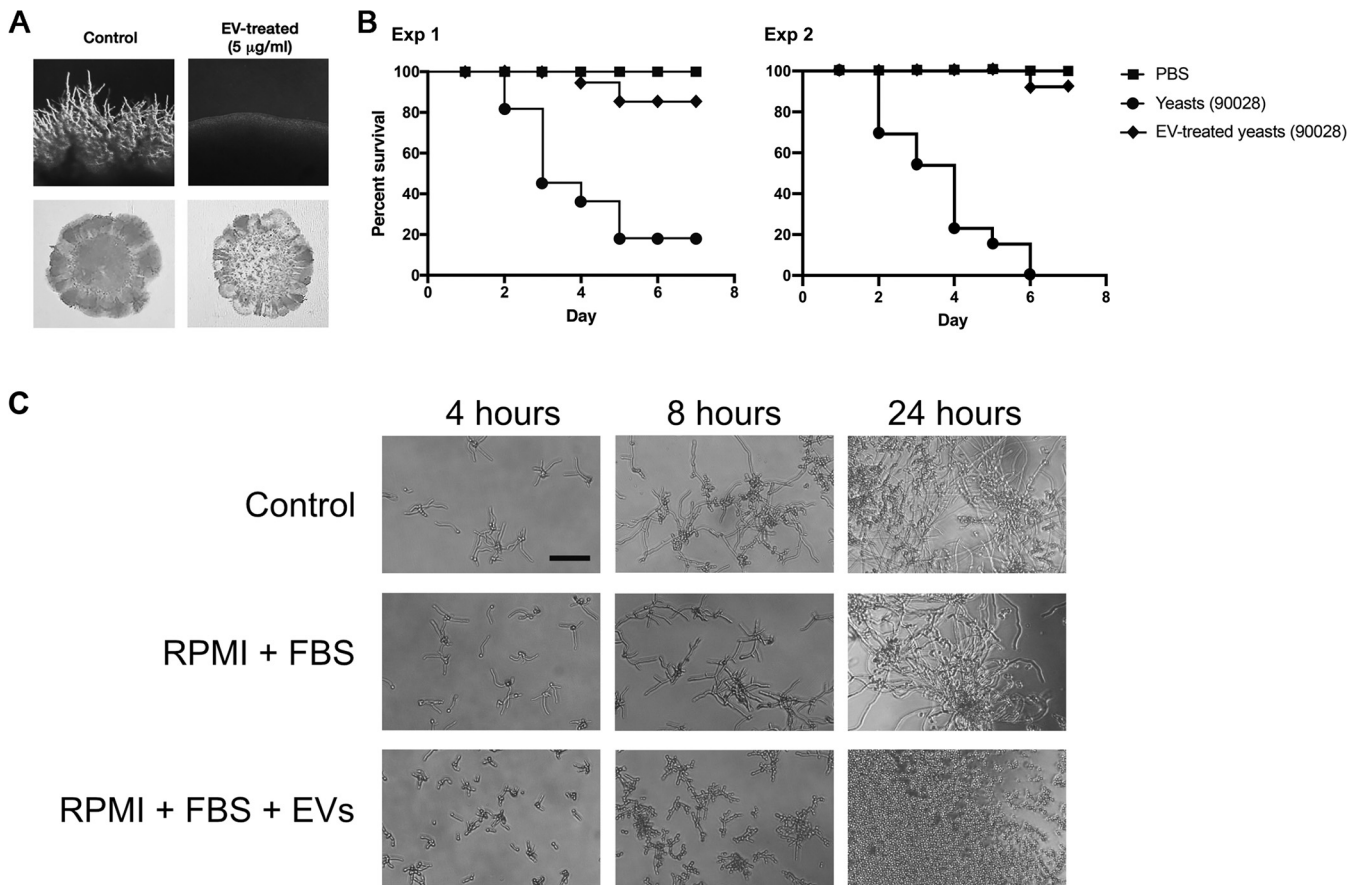


**FIG 8** *C. albicans* EVs decrease the capacity of *C. albicans* to penetrate agar and attenuate virulence in *Galleria mellonella*. (A) *C. albicans* (90028) yeasts were treated with PBS (control) or *C. albicans* 90028 EVs in PBS (5  $\mu\text{g/ml}$ ) and then plated onto M199 agar for 7 days. The presence of filamentation (top panels) and agar invasion (bottom panels) was observed only under control conditions. (B) *G. mellonella* larvae were infected with  $10^5$  *C. albicans* yeast untreated or pretreated with *C. albicans* 90028 EVs (5  $\mu\text{g/ml}$  for 24 h), and survival was monitored (experiments 1 and 2). PBS indicates uninfected larvae injected with PBS. (C) *C. albicans* (90028) yeasts were inoculated into RPMI supplemented with FBS (10%) in the presence or absence of *C. albicans* EVs in a concentration equivalent to 5  $\mu\text{g}$  sterol/mL.

effect have not been investigated here, but the process could involve epigenetic changes, as reported previously for the white-opaque transition (58). In addition to epigenetic modifications, other changes triggered by *C. albicans* 90028 EVs could also be expected and should also be further investigated. For instance, *C. albicans* EV-treated cells lost their ability to adhere to the plates' wells after 7 h of incubation, suggesting that treatment with *C. albicans* EVs caused alterations on the fungal surface composition. Although the activity of *C. albicans* 90028 EVs was dose dependent, the inhibitory effect was apparently not linked to yeast density in fungal cultures. These data suggest that the *C. albicans* 90028 EV components involved with morphogenesis must reach a threshold concentration to inhibit differentiation, a circumstance that is well-known for the QSM FOH and tyrosol (15, 17). This hypothesis agrees with the ordinary physiological transition between yeast and hyphal forms, which would not occur regularly if EVs or other extracellular regulators were inhibitory at minimum concentrations. Altogether, these results indicate that *C. albicans* EVs carry a group of terpenes and fatty acids able to regulate growth and morphogenesis in *C. albicans*. A recent work published by Bitencourt and colleagues (59) also suggested that fungal EVs could be involved in fungal intraspecies communication and could regulate *C. albicans* dimorphism. However, in contrast with our results, those authors demonstrated that *C. albicans* EVs produced by yeasts induced filamentation, although EVs from hyphae exhibited a more prominent effect. In addition, their experiments also suggested that EVs stimulated *C. albicans* growth, a result not exploited but consistently

observed in our current work. These differences might have resulted from the use by Bitencourt et al. (59) of a distinct *C. albicans* strain (ATCC 64548) and a different culture condition (YPD medium), which could modify the EV composition, as previously reported (60). Moreover, their experimental conditions were limited to 4 h of filamentation, when the morphological impact of EVs was just initiating in our experiments. These contrasting effects reinforce the relevance of further investigating EVs in fungal physiology.

To confirm that *C. albicans* uses EV export as a general mechanism to control yeast growth and morphogenesis *in vitro*, we isolated *C. albicans* EVs from two other *C. albicans* strains with distinct filamentation abilities and virulence profiles and tested their capacity to inhibit yeast-to-hyphae differentiation. Our data revealed that these three different strains of *C. albicans* produced EVs with similar properties, which were also comparable to other fungal EVs, as recently characterized by Reis and colleagues using similar detection approaches with *C. gattii* (46). In addition, small differences in EVs size were observed when the distinct strains were compared, confirming previous data published by our group showing that *C. albicans* strains produced EVs with distinct dimensions (31). Morphological differences of EVs are usually attributed to changes in composition and/or biogenesis pathways. EVs released by the strain 90028 were able to inhibit filamentation of all tested *C. albicans* strains. Furthermore, *C. albicans* EVs from different strains also exhibited the ability to block filamentation of *C. albicans* strain 10231. Thus, the *C. albicans* EVs' capacity of inhibiting yeast-to-hypha differentiation appears to be a conserved mechanism.

A number of compounds carried by fungal EVs could be involved with growth and morphogenesis control, including lipids, proteins, and RNA. The participation of thermolabile molecules was discarded since the filamentation inhibition is observed even when the *C. albicans* EVs are heated. Since lipids are thermostable, these results suggest that a lipid compound could be responsible by the *C. albicans* EV-mediated inhibitory activity. Given that FOH is a lipid that regulates morphogenesis in *C. albicans*, we speculate that this molecule could be the component mediating the yeast-to-hypha inhibitory effect. Nevertheless, FOH is not produced by the *C. albicans* strain 10231 and has never been characterized in *H. capsulatum*. Our TLC results confirm the presence of an FOH band with inhibitory activity in *C. albicans* strain 90028, but not in *H. capsulatum* or *S. cerevisiae* lipid extracts. However, it is possible that the colorimetric method used in our experiments was not sufficiently sensitive to detect small amounts of FOH. In addition, it was still necessary to confirm that FOH is addressed to *C. albicans* EVs at appropriate concentrations to inhibit filamentation.

Our GC-MS analysis strongly indicates the presence of lipids in *C. albicans* EVs that could interfere with morphogenesis, including a family of terpenes and medium-chain fatty acids (17, 22). Besides FOH, other sesquiterpenes and diterpenes are major compounds characterized in the *C. albicans* 90028 EVs. Of note, the proportion of terpene species in *C. albicans* EVs is distinct from the LP and displays the largest amounts of FOH isomers. In addition, no FOH has been found in EVs released by the *C. albicans* strain 10231, *S. cerevisiae*, and *H. capsulatum*, which may explain why they have a distinct kinetic to inhibit differentiation compared to EVs released by *C. albicans* strain 90028.

In previous studies, the inhibitory concentration of FOH affecting *C. albicans* differentiation *in vitro* was shown to be in the range of 1 to 150  $\mu\text{M}$  (19, 21, 53–55, 61). According to our quantitative analysis, the sterol/protein weight ratio was 1:20 (data not shown). Most of our experiments were developed using a sterol concentration of 5  $\mu\text{g/mL}$  of EV suspension, corresponding to a protein concentration of 100  $\mu\text{g/mL}$ . Considering the lowest concentration of FOH used in previous studies (1  $\mu\text{M}$ ), the amount of purified FOH required for yeast-to-hyphae inhibition was 222.3 ng/mL. As demonstrated in Table 2, an EV suspension able to inhibit filamentation contained approximately 11.3 ng/mL of FOH, corresponding to the sum of both Z,E-FOH and E,E-FOH isomers. Thus, it was expected that FOH alone was not fully responsible for the

effect exhibited by *C. albicans* EVs. Supporting this hypothesis, *C. albicans* 10231 EVs retained the ability to inhibit filamentation despite the absence of FOH. These results also suggest that other lipids besides FOH might mediate the filamentation inhibition in *C. albicans*, a premise also supported by the fact that FOH has not been found in EVs from *H. capsulatum* and *S. cerevisiae*. DHFOH, geranylgeraniol, and dihydrogeranylgeraniol were the additional terpenes detected in high concentrations in *C. albicans* 90228 EVs. The fact that DHFOH was the only terpene exhibiting a similar activity to FOH indicates that this molecule may contribute significantly to the inhibitory effect mediated by EVs released from *C. albicans* strain 90028. The biological activity of DHFOH has been previously reported in *in vitro* studies that demonstrated that volatile compounds produced by *C. albicans*, including DHFOH, inhibited the growth of dermatophytes (62). Taken together, our and previous functional and analytical data suggest that a combination of lipid species could mediate the inhibitory activity in *C. albicans*.

As mentioned above, our GC-MS data also revealed the presence of different fatty acids species in fungal EVs, including  $C_{12:0}$ ,  $C_{14:0}$ ,  $C_{16:2}$ ,  $C_{18:0}$ , and  $C_{18:1}$ . Earlier studies have demonstrated that long-chain fatty acids have no effect on *C. albicans* differentiation, including octadecanoic and octadecenoic acids (24), major components in *C. albicans* EVs. Nevertheless, butyric acid, a short-chain fatty acid generated by lactic acid-producing bacteria, inhibits *C. albicans* germination by 40 and 98% when used at 25 and 100 mM, respectively. Recent studies suggest that the biological activity of fatty acids in *C. albicans* could be related to their chain length. Murzyn and colleagues (63) have shown that purified  $C_{10:0}$  inhibited *C. albicans* filamentation and reduced its capacity to adhere and form biofilm. Willems and colleagues (64) have confirmed the inhibitory activities of  $C_{10:0}$  incorporated in lipid emulsions. Notably, in both studies,  $C_{10:0}$  did not suppress yeast growth. The effect of  $C_{14:0}$  on *C. albicans* filamentation, biofilm formation, and virulence has recently been investigated by Prasath and colleagues (23). According to these authors,  $C_{14:0}$  blocked yeast-to-hypha differentiation and biofilm formation without compromising fungal viability. In addition, treatment with this fatty acid impacted ergosterol synthesis, sphingolipid metabolism, multidrug resistance, and oxidative stress. The effect of medium-chain fatty acids over *C. albicans* was investigated by Lee and colleagues (22), and they showed that  $C_{7:0}$ ,  $C_{8:0}$ ,  $C_{9:0}$ ,  $C_{10:0}$ ,  $C_{11:0}$ , and  $C_{12:0}$  negatively affected biofilm formation and filamentation in *C. albicans*. Remarkably,  $C_{14:0}$  was enriched in fungal EVs released by strain 10231, and  $C_{12:0}$  was found in high concentrations in EVs from *S. cerevisiae* and *H. capsulatum*, suggesting that the inhibitory effect mediated by these EVs was at least in part due to these lipids. Moreover, treatment with  $C_{7:0}$  and  $C_{9:0}$  modified the expression of biofilm and hyphal growth-regulating genes in a similar fashion to FOH, suggesting that they share the same regulatory mechanism. However, in the same study, the authors stated that cAMP did not reverse the inhibitory effect of fatty acids, which indicated that other signaling pathways related to hyphal development could be impacted. Our experiments showed that if *C. albicans* yeasts were treated with *C. albicans* 90028 EVs and then db-cAMP was added to the wells, a significant reversion of effect was observed. However, the ability of db-cAMP to reverse the EVs effect was reduced when db-cAMP and EVs were preincubated before addition to the culture. These results strongly indicate that EVs are able to inactivate the db-cAMP. Although this last condition is not expected to occur *in vivo*, it shows that fungal EVs have different ways to impact the extracellular environment.

It has been speculated that the reduced size and round shape of yeast cells make them the putative forms used by *C. albicans* to disseminate in the host. However, this possibility is questionable due to the presence of serum in the blood, which would promptly induce germ tube and hypha formation (57). Our experiments showed that *C. albicans* EVs inhibited yeast-to-hypha transition even in the presence of fetal bovine serum (FBS) and 5% CO<sub>2</sub> atmosphere, indicating that morphogenesis could be controlled by EVs during various phases of infection. This possibility was corroborated by the long-term effect manifested by *C. albicans* EVs *in vitro*. Thus, *C. albicans* EVs would

make hypha-to-yeast differentiation feasible *in vivo*, which could possibly explain how this fungus modulates differentiation to facilitate dissemination.

Based on the results discussed above, we have hypothesized that pretreatment of yeast cells *in vitro* with EVs would also decrease *C. albicans*'s ability to invade host cells and cause disease. This possibility is reinforced by the fact that there was a delay during filamentation in the edge of colonies formed by *C. albicans* EV-treated yeast cells during agar-penetrating growth tests. To correlate the inhibitory effect of *C. albicans* EVs with the decrease in fungal invasion and virulence, we have investigated the ability of pretreated yeast cells to kill *G. mellonella* larvae. Indeed, *C. albicans* EV treatment significantly attenuated the ability of *C. albicans* to cause larvae death. Melanization was only observed in larvae infected with untreated yeasts, confirming stress due to invasive candidiasis. This result indicated that by inhibiting yeast-to-hypha differentiation, *C. albicans* EVs decreased fungal virulence. Similar results have been observed when *C. albicans* was treated with the middle-chain fatty acid C<sub>9:0</sub> using *Caenorhabditis elegans* as a model (23). In addition, this validates the idea that controlling filamentation would be a potential approach as a therapeutic strategy (65).

In conclusion, our results support recent findings showing that fungal EVs can be used as messaging compartments and directly influence biofilm production and morphogenesis. In addition, our study presents the fine structural characterization of previously unknown lipid components. EVs could stabilize the lipids and reduce their susceptibility to being oxidized, a function already suggested for liposomes. We have characterized the major players mediating *C. albicans* yeast-to-hypha differentiation, and further studies are necessary to determine whether these identified lipids in combination could be used to control candidiasis *in vivo*.

## MATERIALS AND METHODS

**Microorganisms and culture conditions.** *C. albicans* ATCC strains 90028, 10231, and SC5314 and the *S. cerevisiae* strain RSY225 were cultivated in Sabouraud at 30°C under agitation (150 rpm) for 48 h. *H. capsulatum* strain G-217B (ATCC 26032) was cultivated in *Histoplasma*-macrophage medium (HMM) at 37°C under agitation (180 rpm). *C. albicans* yeast cells were washed with phosphate-buffered saline (PBS) 3 times, enumerated, and then transferred to medium 199 (M199), pH 4.0 or pH 7.0, RPMI-MOPS (morpholinepropanesulfonic acid) 0.165 M, or RPMI supplemented with 10% fetal bovine serum (FBS) according to the experiments described below.

**Isolation and quantification of EVs.** EVs were isolated following protocols developed by our group (31) with minor adjustments. Briefly, yeast cultures (1 L) from each fungal species were collected after 48 h of growth as described above. Cells and debris were removed by sequential centrifugation steps (4,000 and 15,000 × *g*, 15 min, 4°C). An additional step of filtration using a 0.45-μm membrane filter (Merck Millipore) was used to remove any remaining yeast cells or debris. The supernatant was then concentrated using an Amicon ultrafiltration system (100-kDa cutoff; Millipore) to a final volume of approximately 20 mL. EVs were collected by centrifugation at 100,000 × *g* for 1 h at 4°C. Supernatant was discarded, and the pellet enriched in EVs was washed twice with PBS, pH 7.4, at 100,000 × *g* for 1 h at 4°C.

Alternatively, 300 μL containing 10<sup>7</sup> *C. albicans* yeast cells was plated onto petri dishes containing Sabouraud dextrose agar (SDA). After 24 h of growth, yeast cells were harvested using a cell scraper and transferred to 20 mL of PBS. Cells and debris were removed as described above, the supernatant was filtered using a 0.45-μm membrane filter, and the EVs were collected by centrifugation at 100,000 × *g* for 1 h at 4°C. To isolate EVs from macrophages (RAW 264.7 macrophage-like; ATCC TIB-71) culture medium RPMI supplemented with 10% FBS (400 mL), FBS was ultracentrifuged to remove vesicles present, with 70% cellular confluence, and was collected after 24 h and centrifuged (300 × *g* and 15,000 × *g*, 15 min, 4°C). The same steps of filtration were used, and the EVs were recovered after centrifugation at 100,000 × *g* for 1 h at 4°C.

The presence of EVs was confirmed using dynamic light scattering (DLS) analysis (31) and nanoparticle tracking analysis (NTA) (46). EVs were suspended in 200 μL PBS, and aliquots of 5 to 10 μL were used to perform the sterol quantification. Sterol content was determined using the quantitative fluorometric kit Amplex red sterol assay kit (Molecular Probes, Life Technologies). Protein content was measured using the bicinchoninic acid (BCA) kit (Pierce, Thermo Fisher Scientific). Additionally, aliquots of 5 to 10 μL were also plated onto Sabouraud agar plates to confirm that the preparation was sterile.

**NTA of *C. albicans* EVs.** Nanoparticle tracking analysis (NTA) of fungal EVs was performed on an LM10 nanoparticle analysis system, coupled with a 488-nm laser and equipped with a scientific complementary metal oxide semiconductor (SCMOS) camera and a syringe pump (Malvern Panalytical, Malvern, UK) following the conditions used by Reis and colleagues (46). All samples were 833- to 2,500-fold diluted in filtered PBS and measured within the optimal dilution range of 9 × 10<sup>7</sup> to 2.9 × 10<sup>9</sup> particles/mL. Samples were injected using a syringe pump speed of 50, and three videos of 60 s were captured per sample, with the camera level set to 15, gain set to 3, and viscosity set to that of water (0.954 to



0.955 cP). For data analysis, the gain was set to 10 to 15, and the detection threshold was set to 2 to 3 for all samples. Levels of blur and maximum jump distance were automatically set. The data were acquired and analyzed using the NTA 3.0 software (Malvern Panalytical).

**Biofilm assays.** For biofilm production and quantification, two protocols were used. First, yeast cells were plated onto polystyrene 96-well plates containing M199 ( $10^5$  cells/well) in the presence of different concentrations of EVs (0.5, 1, and 5  $\mu\text{g}/\text{mL}$  based on sterol content). Second, yeasts were plated onto polystyrene 96-well plates containing M199 ( $10^5$  cells/well), and the systems were incubated for 90 min. Then, the nonadherent cells were removed by washing with PBS, and fresh M199 was added containing different concentrations of EVs (0.5, 1, and 5  $\mu\text{g}/\text{mL}$  based on sterol content). For both protocols, PBS was used as negative control. Biofilm was allowed to develop for 24 and 48 h at 37°C and then quantified by the crystal violet method. Briefly, after each time point, the biofilm-coated wells were washed 3 times with PBS, air-dried for 45 min, and stained with 0.4% aqueous crystal violet (100  $\mu\text{L}$ ) for 10 min and washed 3 times with 200  $\mu\text{L}$  of PBS. Then, 100  $\mu\text{L}$  of absolute ethanol was added to the wells, and the systems were incubated for 5 min. The plate was then analyzed using a microplate reader (EL808; BioTek) at the wavelength of 540 nm (66). Tests were performed in triplicate. For scanning electron microscopy, yeast cells were washed three times in PBS, pH 7.2  $\pm$  0.1, to remove planktonic cells and fixed in 2.5% glutaraldehyde type I in 0.1 M sodium cacodylate buffer (pH 7.2  $\pm$  0.1) for 1 h at room temperature. After fixation, cells were washed in 0.1 M sodium cacodylate buffer (pH 7.2  $\pm$  0.1) containing 0.2 M sucrose and 2 mM  $\text{MgCl}_2$ . Then, cells were dehydrated in ethanol (30, 50, and 70%, for 5 min and then 95% and 100% twice for 10 min), subjected to critical point drying in an EM CPD300 (Leica, Wetzlar, Germany), covered with gold sputtering (10  $\pm$  2 nm), and visualized in a Zeiss Auriga 40 (Zeiss, Oberkochen, Germany) microscope operated at 2 kV.

**Yeast-to-hyphae differentiation.** *C. albicans* yeast cells ( $2.5 \times 10^3$ /well) were plated onto 96-well plates containing the hypha-inducing medium M199 or RPMI supplemented with 10% FBS. To test whether the number of yeast cells would influence the EV activity, different suspensions of *C. albicans* were used ( $1.5 \times 10^3$ ,  $2 \times 10^4$ , and  $3.5 \times 10^4$  yeast cells/well). Fungal EVs were added at final concentrations varying from 0.025 to 5  $\mu\text{g}/\text{mL}$  (based on sterol content). For the lipid extracts, activity tests aliquots of 10  $\mu\text{L}$  (equivalent to 5  $\mu\text{g}/\text{mL}$  of EVs) were added to the wells. The purified terpenes DHFOH (Penta, USA) and geranylgeraniol (Sigma-Aldrich, USA), solubilized in 1 mL of ethanol, and ascorbic acid 2,6-dihexadecanoate (TCI America, USA), dissolved in 1 mL of acetone, were added to the wells in different concentrations (please see the figure legends). Plates were incubated at 37°C and 5%  $\text{CO}_2$  for 4, 8, and 24 h. For each time interval, the cells' morphologies were visualized under an Observer Z1 microscope (Carl Zeiss International, Germany), and the images were collected and processed with ImageJ (NIH, US) and Photoshop (Adobe). Time-lapse video microscopies were performed after plating yeast cells of *C. albicans* strain 90028 ( $5 \times 10^3$  yeast cells/well) onto 4-well plates containing 1 mL of M199 medium. A final concentration of 5  $\mu\text{g}/\text{mL}$  of *C. albicans* EVs was added to the wells. PBS was used as control. Samples were placed in a culture chamber with controlled temperature and  $\text{CO}_2$  environment (37°C and 5%, respectively) and attached to a Nikon Eclipse TE300 (Nikon, USA). Phase-contrast images were captured every minute using a Hamamatsu C2400 charge-coupled-device (CCD) camera (Hamamatsu, Japan) connected with a Scion FG7 frame grabber (Scion Corporation, USA). Time-lapse images were taken every 1 min using a Nikon Eclipse TE300 microscope attached to a digital Hamamatsu C11440-10C camera (Hamamatsu, Japan). Movie animations were generated using ImageJ v1.8 software (NIH, US).

**EV lipid extraction.** An aliquot containing 50  $\mu\text{g}/\text{mL}$  of EVs was dried using a SpeedVac vacuum concentrator (Eppendorf), followed by lipid extraction with chloroform (C)/methanol (M)/water (W) (8:4:3 [vol/vol/vol]) according to Nimrichter et al. (67). The pellet containing nonextractable residues and precipitated protein was recovered by centrifugation. Partition was obtained after water addition to the system to reach the proportion C/M/W (8:4:5.6 [vol/vol/vol]). The upper and lower phases and the protein content were dried separately using SpeedVac, suspended in dimethyl sulfoxide (DMSO), and their activity tested as described below. The lower (LPs) and upper phases (UPs) contain lipids with higher and lower polarity, respectively. The interphase was also dried using SpeedVac and suspended in DMSO. Aliquots of each fraction (pellet and lower and upper phases) equivalent to 5  $\mu\text{g}/\text{mL}$  (based on sterol content) of EVs according to previous quantification were tested. The same protocol was used to separate the nonpolar components of Sabouraud medium, and the lower phase was used as control.

**Thermostability of EV activity.** To investigate the thermostability of the *C. albicans* 90028 yeast EV activity, the samples were heated for 15 min at 90°C. Then, a final concentration corresponding to 5  $\mu\text{g}/\text{mL}$  (based on sterol content before heat treatment) of EVs was tested as described above.

**Long-term effect of EVs.** *C. albicans* yeast cells ( $2.5 \times 10^3$ /well) were plated onto 96-well plates containing M199 and treated with 5  $\mu\text{g}/\text{mL}$  (based on sterol content) of EVs. The cell morphology of *C. albicans* was analyzed using an Observer Z1 microscope (Carl Zeiss International, Germany) after 4, 8, and 24 h. The yeast cells were collected after 24 h of incubation in the presence of EVs and washed three times with PBS. Yeast cells were enumerated, and a total of  $2.5 \times 10^3$ /well were transferred to fresh M199 in the absence of EVs. These steps were repeated four times without addition of EVs to the cultures. Untreated yeast cells cultivated in M199 were used as control every 24 h. These steps were repeated four times.

**Hyphae-to-yeast differentiation.** Yeast cells of *C. albicans* ( $2.5 \times 10^3$ /well) were plated onto 96-well plates containing M199 media and then incubated for 4 h to allow yeast-to-hypha differentiation. After this period, 100% of the yeast cells differentiated to hyphae. Then, a final concentration of EVs (5  $\mu\text{g}/\text{mL}$ , based on sterol content), EVs (5  $\mu\text{g}/\text{mL}$ ), FOH (80, 8 and 0.8  $\mu\text{M}$ ), and DHFOH (80, 8 and 0.8  $\mu\text{M}$ ) were added to the wells and the morphology accompanied for additional 4, 8, and 24 h as described above. PBS was used as control. Tyrosol stock was diluted in methanol.

**db-cAMP effect on EV inhibitory activity.** Yeast cells of *C. albicans* ( $2.5 \times 10^3$ /well) were plated onto 96-well plates containing M199 and treated with  $5 \mu\text{g}/\text{mL}$  (based on sterol content) of *C. albicans* 90028 EVs preincubated with the cAMP donor db-cAMP (10 mM) (Sigma-Aldrich) for 1 h. Alternatively, yeasts were treated with *C. albicans* 90028 EVs for 1 h, and then db-cAMP (10 mM) was added to the wells. Cell morphology was analyzed using an Observer Z1 microscope (Carl Zeiss International, Germany) after 4, 8, and 24 h.

**Yeast lipid extraction.** Yeast of *C. albicans*, *H. capsulatum*, and *S. cerevisiae* ( $6 \times 10^{10}$  cells) was suspended in a mixture of C/M (2:1 [vol/vol]), stirred for 16 h at room temperature, and then clarified by centrifugation. Cells were extracted with a mixture of C and M (1:2 [vol/vol]) under the same conditions. Lipid extracts were combined and dried using a rotavapor (Heidolph, Germany). The lipids were then suspended in a mixture of C/M/W (8:4:5.6 [vol/vol]) and vigorously mixed. The lower phase was dried using a rotavapor and suspended in 2.5 mL of chloroform. Aliquots were dried using Vacufuge Plus vacuum concentrator (Eppendorf, Germany) and suspended in DMSO. A yeast-to-hypha differentiation assay was performed to determine the minimal amount of the lower phase from *C. albicans* (20, 4, 2, 1, 0.5, 0.25, 0.125, and 0.05 mg/mL) was able to block the differentiation.

**Size exclusion chromatography.** To exclude the presence of free-contaminants in EV preparations, we used size exclusion chromatography (SEC) according to Menezes-Neto and colleagues (68) with minor adjustments. Briefly, Sepharose 4B (final volume of 10 mL) was packed in a 10-mL syringe and then equilibrated with PBS-citrate 0.36% (wt/vol). The EVs obtained after ultracentrifugation were suspended in a final volume of 500  $\mu\text{L}$  and applied to the column. A total of 30 fractions of 500  $\mu\text{L}$  were collected immediately after column loading using PBS-citrate as eluant. EVs aliquots of 5 to 10  $\mu\text{L}$  were used to perform the sterol and protein quantification as described previously. A yeast-to-hypha differentiation assay was performed to determine the activity of each fraction. To avoid additional steps to concentrate the samples, the lipids from each fraction were extracted as described above and the LP normalized according to the sterol content. A final concentration of  $5 \mu\text{g}/\text{mL}$  of sterol was used. For the fractions where sterol was not detected, 400  $\mu\text{L}$  of each fraction was used for lipid extraction and solvent partition. The LP was dried down in a SpeedVac and suspended in 2  $\mu\text{L}$  of DMSO. An aliquot of 1  $\mu\text{L}$  was used to test the inhibitory activity.

**Reverse-phase thin-layer chromatography.** EVs or LP lipids were suspended in C/M (1:1 [vol/vol]), and their concentration was normalized by sterol content or the total weight, respectively. Aliquots of 10  $\mu\text{L}$  were spotted into reverse-phase TLC (RP-TLC) plates (silica gel 60 RP-18 F254; 1 mm; Merck, Germany). The plates were developed in chambers presaturated for 10 min using acetone as a solvent system. After development, plates were dried at room temperature, and the bands were visualized after spraying with a solution of 50 mg ferric chloride ( $\text{FeCl}_3$ ) in a mixture of 90 mL water, 5 mL acetic acid, and 5 mL sulfuric acid (69). After spraying, plates were heated at  $100^\circ\text{C}$  for 3 to 5 min. FOH was used as standard. Under these conditions, FOH appears as a purple band. Alternatively, the developed plates were incubated in a saturated iodine chamber where the lipids appear as yellow bands. The bands were scraped from the TLC and placed into microcentrifuge tubes. Lipids were suspended in C/M (1:1 [vol/vol]) and filtered using a polyvinylidene difluoride (PVDF) membrane with 0.22  $\mu\text{m}$  to a new microcentrifuge tube. Samples were dried down using a SpeedVac, suspended in DMSO, and normalized by lipid weight. For the lipid activity tests, aliquots of 10  $\mu\text{L}$  (equivalent to  $5 \mu\text{g}/\text{mL}$  of EVs) were added to the wells containing yeasts of *C. albicans* in M199 medium. Plates were incubated at  $37^\circ\text{C}$  and 5%  $\text{CO}_2$  for 4, 8, and 24 h. For each time point, the cells' morphologies were visualized under an Observer Z1 microscope (Carl Zeiss International, Germany), and the images were collected and processed with ImageJ (NIH, USA) and Photoshop (Adobe).

**FOH extraction.** The *C. albicans* yeast 90028 and 10231 EV samples (19.1  $\mu\text{g}$  total sterol) were resuspended in 400  $\mu\text{L}$  methanol (high-performance liquid chromatography [HPLC] grade; Fisher Scientific), vortexed for 2 min, and centrifuged for 15 min at  $14,000 \times g$  at room temperature. The supernatants were transferred to a 2-mL polytetrafluoroethylene (PTFE)-lined cap glass tube (Supelco; catalog no. 27134; Sigma-Aldrich). The ensuing pellet was redissolved in 400  $\mu\text{L}$  methanol, and the previous steps were repeated. The two resulting supernatants were pooled and dried under nitrogen gas in Supelco PTFE-lined cap glass vials. For FOH extraction, the yeast *C. albicans* yeast 90028 and 10231 EV samples were partitioned by adding 500  $\mu\text{L}$  HPLC-grade water (Fisher Scientific) and 500  $\mu\text{L}$  ethyl acetate (Sigma-Aldrich; catalog no. 270989) and vortexed for 2 min. After phase separation, the upper (organic) phase was collected, transferred to a fresh PTFE-lined cap glass vial, and dried under nitrogen gas. Samples were then redissolved in 20  $\mu\text{L}$  methylene chloride (Optima grade, Fisher Scientific), transferred to Verex PTFE-lined/silicone cap vials (Phenomenex;  $\mu\text{Vial i3}$  [Qsert]) just prior to gas chromatography-mass spectrometry (GC-MS) analysis.

**Lipid analysis by GC-MS.** A standard of FOH isomer mixture (catalog no. 93547; Supelco, Sigma-Aldrich) was diluted in methylene chloride (Optima grade, Fisher Scientific) to a concentration of 22.5 pmol/ $\mu\text{L}$  to determine the transition ions to be used in the selected-reaction monitoring (SRM) method. Chromatographic separation was performed by injecting 1  $\mu\text{L}$  of FOH standard onto a Thermo TSQ 9000 triple-quadrupole GC-MS/MS system (Thermo Fisher Scientific) set to splitless, MS transfer line at  $250^\circ\text{C}$ , with an AI/AS 1310 series autosampler (Thermo Fisher Scientific), equipped with a Zebron (ZB-FFAP; 30-m by 0.32-mm by 0.25- $\mu\text{m}$ ) column, previously indicated for separation of FOH isomers (51). Isomers were separated by maintaining a loading temperature of  $40^\circ\text{C}$  for 1.2 min, followed by a heat gradient to  $250^\circ\text{C}$  at a rate of  $20^\circ\text{C}/\text{min}$ , and a plateau held at  $250^\circ\text{C}$  until the end of the run at 13.5 min. Additionally, ramped pressure was applied throughout the run, beginning with 89 kPa held for 2 min, and increased to 150 kPa over 6.1 min, while holding at 150 kPa until the end of the run. Initially, a full scan was run to determine the retention time (RT) and underivatized FOH limits of detection prior to FOH SRM confirmation and full scan analysis.

The lowest detectable level of underivatized FOH isomers from the standard, using the automated SRM (AutoSRM) mode on the TSQ 9000 triple-quadrupole GC-MS (Thermo Fisher Scientific) with an electron

ionization (EI) source temperature of 320°C, was 4.5 fmol/μL. However, subsequent analyses were performed with a concentration of FOH standard of 4.5 pmol/μL, in which the detection of all four isomers (Z, Z, Z,E, E,Z, and E,E) of FOH was reproducible, and the signal of the least abundant isomer (Z,Z) was at least ~10% of the most abundant (E,E) isomer and ~6-fold higher than the background. Using the AutoSRM mode on the TSQ 9000 GC-MS dashboard feature, the ion fragmentation was optimized at their respective RT with the top three transition ions (81.1 to 79.1 at 8 collision energy [CE], 69.1 to 41 at 6 CE, and 41.1 to 39.1 at 8 CE) were chosen and imported into Chromeleon v7.2.9 software. Images of the SRM chromatograms of the FOH standard and the samples extracted from *C. albicans* yeast 90028 and *C. albicans* 10231 EVs were transferred from Chromeleon v7.2.9 into PowerPoint for figure generation.

**Quantitative analysis of FOH or FOH-like molecules by GC-MS.** FOH quantitation was performed by building a standard curve with d6-E,E-FOH (catalog no. SKU7002940; Avanti Polar Lipids, Alabaster, AL) at concentrations of 0.1, 1, 2.5, and 5 ng/μL. Peak areas of the standard and samples were imported into GraphPad Prism 9.0.0 for formula and  $R^2$  generation and graph.

**Agar invasion assay.** Hyphal growth was stimulated using M199 medium. *C. albicans* (90028) yeast cells were treated or not with EVs (5 μg/mL, based on sterol content) overnight, and a suspension of yeast cells 10 μL containing 10<sup>5</sup> cells was plated onto M199 agar plates. Plates were then incubated at 37°C, and growth was monitored daily for hypha formation. After 10 days of incubation, colonies were washed in a stream of water using the same flow rate, water temperature, and duration of time as described by Cullen (56). Colony images were taken with an Optiphase microscope coupled with a digital camera (AmScope) and processed using Adobe Photoshop.

**Galleria mellonella infection.** Larvae of wax moth *G. mellonella* were used to investigate virulence of EV-treated yeast cells (70). *C. albicans* yeast cells ( $2.5 \times 10^3$ ) were treated with EVs (5 μg/mL, based on sterol content) in M199 for 24 h. Yeast cells were then washed in PBS and enumerated. As a control, yeast cells cultivated in Sabouraud were used. A final volume of 10 μL containing  $2 \times 10^5$  yeast cells was injected into the last right proleg of the larvae (200 to 300 mg each) using a Hamilton syringe. An additional control included larvae injected with 10 μL PBS alone. The injected larvae were kept at 37°C, and the number of deceased subjects per group was monitored daily.

**Statistical analysis.** All statistical analyses were performed using GraphPad Prism 6 v5.02 for Windows (GraphPad Software).

Supplemental material can be found at [10.6084/m9.figshare.19403894](https://doi.org/10.6084/m9.figshare.19403894).

## ACKNOWLEDGMENTS

This work was supported by grants from the Brazilian agency Conselho Nacional de Desenvolvimento Científico e Tecnológico (CNPq; grants 405520/2018-2, 440015/2018-9, and 301304/2017-3 to M.L.R.; 311179/2017-7 and 408711/2017-7 to L.N.; and 311470/2018-1 to A.J.G.), FAPERJ (E-26/202.809/2018 to L.N. and E-26/202.696/2018 and E-26/202.760/2015 to A.J.G.), FIOCRUZ (grants VPPCB-007-FIO-18 and VPPIS-001-FIO18), and Coordenação de Aperfeiçoamento de Pessoal de Nível Superior (CAPES, Finance Code 001). J.D.N. was supported in part by NIH R21 AI124797. This work was also supported in part by NIH grants AI136934, AI116420, and AI125770 and in part by Merit Review Grant I01BX002924 from the Veterans Affairs Program to MDP. I.C.A. was partially supported by grant number U54MD007592 from the National Institute on Minority Health and Health Disparities (NIMHD), a component of the National Institutes of Health (NIH).

We thank the Biomolecule Analysis and Omics Unit at the Border Biomedical Research Center, UTEP, supported by NIMHD grant number U54MD007592 (to Robert A. Kirken), for the access to the GC-MS and other instruments.

M.T.M. received a Ph.D. fellowship from the Science Without Borders Program, sponsored by the Capes Foundation within the Ministry of Education, Brazil (grant no. BEX 013622/2013-07).

Maurizio Del Poeta, M.D. is a cofounder and chief scientific officer (CSO) of MicroRid Technologies Inc.

## REFERENCES

- Kühbacher A, Burger-Kentischer A, Rupp S. 2017. Interaction of *Candida* species with the skin. *Microorganisms* 5:32. <https://doi.org/10.3390/microorganisms5020032>.
- Ranjan A, Dongari-Bagtzoglou A. 2018. Tipping the balance: *C. albicans* adaptation in polymicrobial environments. *JoF* 4:112. <https://doi.org/10.3390/jof4030112>.
- Zhang S-L, Wang S-N, Miao C-Y. 2017. Influence of microbiota on intestinal immune system in ulcerative colitis and its intervention. *Front Immunol* 8:1674. <https://doi.org/10.3389/fimmu.2017.01674>.
- Höfs S, Mogavero S, Hube B. 2016. Interaction of *Candida albicans* with host cells: virulence factors, host defense, escape strategies, and the microbiota. *J Microbiol* 54:149–169. <https://doi.org/10.1007/s12275-016-5514-0>.
- Basso V, d'Enfert C, Znaidi S, Bachellier-Bassi S. 2018. From genes to networks: the regulatory circuitry controlling *Candida albicans* morphogenesis. *Curr Top Microbiol Immunol* 18:61–99. [https://doi.org/10.1007/82\\_2018\\_144](https://doi.org/10.1007/82_2018_144).
- Hall RA. 2017. Adapting to change: interactions of *Candida albicans* with its environment. *Future Microbiol* 12:931–934. <https://doi.org/10.2217/fmb-2017-0130>.
- Gauthier GM. 2015. Dimorphism in fungal pathogens of mammals, plants, and insects. *PLoS Pathog* 11:e1004608. <https://doi.org/10.1371/journal.ppat.1004608>.

8. Cassone A, Sullivan PA, Shepherd MG. 1985. N-acetyl-D-glucosamine-induced morphogenesis in *Candida albicans*. *Microbiologica* 8:85–99.
9. Csanik C, Schröppel K, Leberer E, Harcus D, Mohamed O, Meloche S, Thomas DY, Whiteway M. 1998. Roles of the *Candida albicans* mitogen-activated protein kinase homolog, Cek1p, in hyphal development and systemic candidiasis. *Infect Immun* 66:2713–2721. <https://doi.org/10.1128/IAI.66.6.2713-2721.1998>.
10. Maidan MM, Thevelein JM, Van Dijck P. 2005. Carbon source induced yeast-to-hypha transition in *Candida albicans* is dependent on the presence of amino acids and on the G-protein-coupled receptor Gpr1. *Biochem Soc Trans* 33:291–293. <https://doi.org/10.1042/BST0330291>.
11. Seeley WW. 2009. Fungal adenylyl cyclase integrates CO<sub>2</sub> sensing with cAMP signaling and virulence. *Curr Biol* 27:2349–2356. <https://doi.org/10.1016/j.cub.2005.10.040>.
12. Gow NAR, van de Veerdonk FL, Brown AJP, Netea MG. 2011. *Candida albicans* morphogenesis and host defence: discriminating invasion from colonization. *Nat Rev Microbiol* 10:112–122. <https://doi.org/10.1038/nrmicro2711>.
13. Padder SA, Prasad R, Shah AH. 2018. Quorum sensing: a less known mode of communication among fungi. *Microbiol Res* 210:51–58. <https://doi.org/10.1016/j.micres.2018.03.007>.
14. Mallick EM, Bennett JR. 2013. Sensing of the microbial neighborhood by *Candida albicans*. *PLoS Pathog* 9:e1003661. <https://doi.org/10.1371/journal.ppat.1003661>.
15. Chen H, Fujita M, Feng Q, Clardy J, Fink GR. 2004. Tyrosol is a quorum-sensing molecule in *Candida albicans*. *Proc Natl Acad Sci U S A* 101:5048–5052. <https://doi.org/10.1073/pnas.0401416101>.
16. Oh K-B, Miyazawa H, Naito T, Matsuoka H. 2001. Purification and characterization of an autoregulatory substance capable of regulating the morphological transition in *Candida albicans*. *Proc Natl Acad Sci U S A* 98:4664–4668. <https://doi.org/10.1073/pnas.071404698>.
17. Hornby JM, Jensen EC, Liscic AD, Tasto JJ, Jahnke B, Shoemaker R, Dussault P, Nickerson KW. 2001. Quorum sensing in the dimorphic fungus *Candida albicans* is mediated by farnesol. *Appl Environ Microbiol* 67:2982–2992. <https://doi.org/10.1128/AEM.67.7.2982-2992.2001>.
18. Kruppa M. 2009. Quorum sensing and *Candida albicans*. *Mycoses* 52:1–10. <https://doi.org/10.1111/j.1439-0507.2008.01626.x>.
19. Riekhof WR, Nickerson KW. 2017. Quorum sensing in *Candida albicans*: farnesol versus farnesoic acid. *FEBS Lett* 591:1637–1640. <https://doi.org/10.1002/1873-3468.12694>.
20. Albuquerque P, Casadevall A. 2012. Quorum sensing in fungi—a review. *Med Mycol* 50:337–345. <https://doi.org/10.3109/13693786.2011.652201>.
21. Ramage G, Saville SP, Wickes BL, López-Ribot JL. 2002. Inhibition of *Candida albicans* biofilm formation by farnesol, a quorum-sensing molecule. *Appl Environ Microbiol* 68:5459–5463. <https://doi.org/10.1128/AEM.68.11.5459-5463.2002>.
22. Lee J-H, Kim Y-G, Khadke SK, Lee J. 2021. Antibiofilm and antifungal activities of medium-chain fatty acids against *Candida albicans* via mimicking of the quorum-sensing molecule farnesol. *Microb Biotechnol* 14:1353–1366. <https://doi.org/10.1111/1751-7915.13710>.
23. Prasath KG, Sethupathy S, Pandian SK. 2019. Proteomic analysis uncovers the modulation of ergosterol, sphingolipid and oxidative stress pathway by myristic acid impeding biofilm and virulence in *Candida albicans*. *J Proteomics* 208:103503. <https://doi.org/10.1016/j.jprot.2019.103503>.
24. Noverr MC, Huffnagle GB. 2004. Regulation of *Candida albicans* morphogenesis by fatty acid metabolites. *Infect Immun* 72:6206–6210. <https://doi.org/10.1128/IAI.72.11.6206-6210.2004>.
25. Rodrigues ML, Nimrichter L, Oliveira DL, Frases S, Miranda K, Zaragoza O, Alvarez M, Nakouzi A, Feldmesser M, Casadevall A. 2007. Vesicular polysaccharide export in *Cryptococcus neoformans* is a eukaryotic solution to the problem of fungal trans-cell wall transport. *Eukaryot Cell* 6:48–59. <https://doi.org/10.1128/EC.00318-06>.
26. Rodrigues ML, Nosanchuk JD, Schrank A, Vainstein MH, Casadevall A, Nimrichter L. 2011. Vesicular transport systems in fungi. *Future Microbiol* 6:1371–1381. <https://doi.org/10.2217/fmb.11.112>.
27. Rodrigues MLML, Franzen AJAJ, Nimrichter L, Miranda K. 2013. Vesicular mechanisms of traffic of fungal molecules to the extracellular space. *Curr Opin Microbiol* 16:414–420. <https://doi.org/10.1016/j.mib.2013.04.002>.
28. Vallejo MC, Matsuo AL, Ganiko L, Medeiros LCS, Miranda K, Silva LS, Freymüller-Haapalainen E, Sinagaglia-Coimbra R, Almeida IC, Puccia R. 2011. The pathogenic fungus *Paracoccidioides brasiliensis* exports extracellular vesicles containing highly immunogenic  $\alpha$ -galactosyl epitopes. *Eukaryot Cell* 10:343–351. <https://doi.org/10.1128/EC.00227-10>.
29. Bielska E, Sisuquella MA, Aldeieg M, Birch C, O'Donoghue EJ, May RC. 2018. Pathogen-derived extracellular vesicles mediate virulence in the fatal human pathogen *Cryptococcus gattii*. *Nat Commun* 9:1556. <https://doi.org/10.1038/s41467-018-03991-6>.
30. Rodrigues ML, Oliveira DL, Vargas G, Girard-Dias W, Franzen AJ, Frases S, Miranda K, Nimrichter L. 2016. Analysis of yeast extracellular vesicles. *Methods Mol Biol* 1459:175–190. [https://doi.org/10.1007/978-1-4939-3804-9\\_12](https://doi.org/10.1007/978-1-4939-3804-9_12).
31. Vargas G, Rocha JDB, Oliveira DL, Albuquerque PC, Frases S, Santos SS, Nosanchuk JD, Gomes AMO, Medeiros LCAS, Miranda K, Sobreira TJP, Nakayasu ES, Arigi EA, Casadevall A, Guimaraes AJ, Rodrigues ML, Freire-de-Lima CG, Almeida IC, Nimrichter L. 2015. Compositional and immunobiological analyses of extracellular vesicles released by *Candida albicans*. *Cell Microbiol* 17:389–407. <https://doi.org/10.1111/cmi.12374>.
32. Baltazar LM, Zamith-Miranda D, Burnet MC, Choi H, Nimrichter L, Nakayasu ES, Nosanchuk JD. 2018. Concentration-dependent protein loading of extracellular vesicles released by *Histoplasma capsulatum* after antibody treatment and its modulatory action upon macrophages. *Sci Rep* 8:8065. <https://doi.org/10.1038/s41598-018-25665-5>.
33. Nimrichter L, de Souza MM, Del Poeta M, Nosanchuk JD, Joffe L, Tavares P, d M, Rodrigues ML. 2016. Extracellular vesicle-associated transitory cell wall components and their impact on the interaction of fungi with host cells. *Front Microbiol* 7:1034. <https://doi.org/10.3389/fmicb.2016.01034>.
34. Oliveira DL, Freire-de-Lima CG, Nosanchuk JD, Casadevall A, Rodrigues ML, Nimrichter L. 2010. Extracellular vesicles from *Cryptococcus neoformans* modulate macrophage functions. *Infect Immun* 78:1601–1609. <https://doi.org/10.1128/IAI.01171-09>.
35. Rodrigues ML, Nakayasu ES, Oliveira DL, Nimrichter L, Nosanchuk JD, Almeida IC, Casadevall A. 2008. Extracellular vesicles produced by *Cryptococcus neoformans* contain protein components associated with virulence. *Eukaryot Cell* 7:58–67. <https://doi.org/10.1128/EC.00370-07>.
36. Rodrigues ML, Nimrichter L, Oliveira DL, Nosanchuk JD, Casadevall A. 2008. Vesicular trans-cell wall transport in fungi: a mechanism for the delivery of virulence-associated macromolecules? *Lipid Insights* 2:LPI.S1000. <https://doi.org/10.4137/LPI.S1000>.
37. Ikeda MAK, de Almeida JRF, Jannuzzi GP, Cronemberger-Andrade A, Torrecilhas ACT, Moretti NS, da Cunha JPC, de Almeida SR, Ferreira KS. 2018. Extracellular vesicles from *Sporothrix brasiliensis* are an important virulence factor that induce an increase in fungal burden in experimental sporotrichosis. *Front Microbiol* 9:2286. <https://doi.org/10.3389/fmicb.2018.02286>.
38. Rayner S, Bruhn S, Vallhov H, Andersson A, Billmyre RB, Scheynius A. 2017. Identification of small RNAs in extracellular vesicles from the commensal yeast *Malassezia sympodialis*. *Sci Rep* 7:39742–39749. <https://doi.org/10.1038/srep39742>.
39. Rizzo J, Chaze T, Miranda K, Roberson RW, Gorgette O, Nimrichter L, Matondo M, Latgé J-P, Beauvais A, Rodrigues ML. 2020. Characterization of extracellular vesicles produced by *Aspergillus fumigatus* protoplasts. *mSphere* 5:e00476-20. <https://doi.org/10.1128/mSphere.00476-20>.
40. Eisenman HC, Frases S, Nicola AM, Rodrigues ML, Casadevall A. 2009. Vesicle-associated melanization in *Cryptococcus neoformans*. *Microbiology (Reading)* 155:3860–3867. <https://doi.org/10.1099/mic.0.032854-0>.
41. Piffer AC, Kuczera D, Rodrigues ML, Nimrichter L. 2021. The paradoxical and still obscure properties of fungal extracellular vesicles. *Mol Immunol* 135:137–146. <https://doi.org/10.1016/j.molimm.2021.04.009>.
42. Huang S-H, Wu C-H, Chang YC, Kwon-Chung KJ, Brown RJ, Jong A. 2012. *Cryptococcus neoformans*-derived microvesicles enhance the pathogenesis of fungal brain infection. *PLoS One* 7:e48570. <https://doi.org/10.1371/journal.pone.0048570>.
43. Costa JH, Bazioli JM, Barbosa LD, dos Santos Júnior PLT, Reis FCG, Klimeck T, Crnkovic CM, Berlinck RGS, Sussulini A, Rodrigues ML, Fill TP. 2021. Phytotoxic tryptoquialanines produced in vivo by *Penicillium digitatum* are exported in extracellular vesicles. *mBio* 12:e03393-20. <https://doi.org/10.1128/mBio.03393-20>.
44. Zarnowski R, Sanchez R, Covelli AS, Dominguez E, Jaromin A, Bernhardt J, Mitchell KF, Heiss C, Azadi P, Mitchell A, Andes DR. 2018. *Candida albicans* biofilm-induced vesicles confer drug resistance through matrix biogenesis. *PLoS Biol* 16:e2006872. <https://doi.org/10.1371/journal.pbio.2006872>.
45. Zarnowski R, Noll A, Chevrette MG, Sanchez H, Jones R, Anhalt H, Fossen J, Jaromin A, Currie C, Nett JE, Mitchell A, Andes DR. 2021. Coordination of fungal biofilm development by extracellular vesicle cargo. *Nat Commun* 12:6235. <https://doi.org/10.1038/s41467-021-26525-z>.
46. Reis FCG, Borges BS, Jozefowicz LJ, Sena BAG, Garcia AWA, Medeiros LC, Martins ST, Honorato L, Schrank A, Vainstein MH, Krmetzsch L, Nimrichter L, Alves LR, Staats CC, Rodrigues ML. 2019. A novel protocol for the isolation of fungal extracellular vesicles reveals the participation of a putative scramblase in polysaccharide export and capsule construction in

- Cryptococcus gattii*. mSphere 4:e00080-19. <https://doi.org/10.1128/mSphere.00080-19>.
47. Thewes S, Moran GP, Magee BB, Schaller M, Sullivan DJ, Hube B. 2008. Phenotypic screening, transcriptional profiling, and comparative genomic analysis of an invasive and non-invasive strain of *Candida albicans*. BMC Microbiol 8:187. <https://doi.org/10.1186/1471-2180-8-187>.
  48. Svennerholm L, Fredman P. 1980. A procedure for the quantitative isolation of brain gangliosides. Biochim Biophys Acta 617:97–109. [https://doi.org/10.1016/0005-2760\(80\)90227-1](https://doi.org/10.1016/0005-2760(80)90227-1).
  49. Hock R, Benda I, Schreier P. 1984. Formation of terpenes by yeasts during alcoholic fermentation. Z Lebensm Unters Forch 179:450–452. <https://doi.org/10.1007/BF01043423>.
  50. DeBarber AE, Bleye LA, Roulet J-BO, Koop DR. 2004.  $\omega$ -Hydroxylation of farnesol by mammalian cytochromes P450. Biochim Biophys Acta 1682: 18–27. <https://doi.org/10.1016/j.bbali.2004.01.003>.
  51. Lee H, Finckbeiner S, Yu JS, Wiemer DF, Eisner T, Attygalle AB. 2007. Characterization of (E,E)-farnesol and its fatty acid esters from anal scent glands of nutria (*Myocastor coypus*) by gas chromatography–mass spectrometry and gas chromatography–infrared spectrometry. J Chromatography A 1165:136–143. <https://doi.org/10.1016/j.chroma.2007.06.041>.
  52. Clément M, Tremblay J, Lange M, Thibodeau J, Belhumeur P. 2007. Whey-derived free fatty acids suppress the germination of *Candida albicans* in vitro. FEMS Yeast Res 7:276–285. <https://doi.org/10.1111/j.1567-1364.2006.00166.x>.
  53. Puppuluri P, Mekala S, Chaffin WL. 2007. Farnesol-mediated inhibition of *Candida albicans* yeast growth and rescue by a diacylglycerol analogue. Yeast 24:681–693. <https://doi.org/10.1002/yea.1501>.
  54. Lindsay AK, Deveau A, Piispanen AE, Hogan DA. 2012. Farnesol and cyclic AMP signaling effects on the hypha-to-yeast transition in *Candida albicans*. Eukaryot Cell 11:1219–1225. <https://doi.org/10.1128/EC.00144-12>.
  55. Davis-Hanna A, Piispanen AE, Stateva LI, Hogan DA. 2008. Farnesol and dodecanol effects on the *Candida albicans* Ras1-cAMP signalling pathway and the regulation of morphogenesis. Mol Microbiol 67:47–62. <https://doi.org/10.1111/j.1365-2958.2007.06013.x>.
  56. Cullen PJ. 2015. The plate-washing assay: a simple test for filamentous growth in budding yeast. Cold Spring Harb Protoc 2015:168–171. <https://doi.org/10.1101/pdb.prot085068>.
  57. Mattia E, Carruba G, Angiolella L, Cassone A. 1982. Induction of germ tube formation by N-acetyl-D-glucosamine in *Candida albicans*: uptake of inducer and germinative response. J Bacteriol 152:555–562. <https://doi.org/10.1128/jb.152.2.555-562.1982>.
  58. Lohse MB, Johnson AD. 2010. Temporal anatomy of an epigenetic switch in cell programming: the white-opaque transition of *C. albicans*. Mol Microbiol 78:331–343. <https://doi.org/10.1111/j.1365-2958.2010.07331.x>.
  59. Bitencourt TA, Hatanaka O, Personi AM, Freitas MS, Trentin G, Santos P, Rossi A, Martinez-Rossi NM, Alves LL, Casadevall A, Rodrigues ML, Almeida F. 2022. Fungal extracellular vesicles are involved in intraspecies intracellular communication. mBio 13:e03272-21. <https://doi.org/10.1128/mbio.03272-21>.
  60. Cleare LG, Zamith D, Heyman HM, Couvillion SP, Nimrichter L, Rodrigues ML, Nakayasu ES, Nosanchuk JD. 2020. Media matters! Alterations in the loading and release of *Histoplasma capsulatum* extracellular vesicles in response to different nutritional milieus. Cell Microbiol 22:e13217. <https://doi.org/10.1111/cmi.13217>.
  61. Mosel DD, Dumitru R, Hornby JM, Atkin AL, Nickerson KW. 2005. Farnesol concentrations required to block germ tube formation in *Candida albicans* in the presence and absence of serum. Appl Environ Microbiol 71: 4938–4940. <https://doi.org/10.1128/AEM.71.8.4938-4940.2005>.
  62. Brasch J, Horter F, Fritsch D, Beck-Jendroschek V, Tröger A, Francke W. 2014. Acyclic sesquiterpenes released by *Candida albicans* inhibit growth of dermatophytes. Med Mycol 52:46–55. <https://doi.org/10.3109/13693786.2013.814174>.
  63. Murzyn A, Krasowska A, Stefanowicz P, Dziadkowiec D, Łukaszewicz M. 2010. Capric acid secreted by *S. boulardii* inhibits *C. albicans* filamentous growth, adhesion and biofilm formation. PLoS One 5:e12050. <https://doi.org/10.1371/journal.pone.0012050>.
  64. Willems HME, Stultz JS, Coltrane ME, Fortwendel JP, Peters BM. 2019. Disparate *Candida albicans* biofilm formation in clinical lipid emulsions due to capric acid-mediated inhibition. Antimicrob Agents Chemother 63: e01394-19. <https://doi.org/10.1128/AAC.01394-19>.
  65. Jacobsen ID, Wilson D, Wächtler B, Brunke S, Naglik JR, Hube B. 2012. *Candida albicans* dimorphism as a therapeutic target. Expert Rev Anti Infect Ther 10:85–93. <https://doi.org/10.1586/eri.11.152>.
  66. Jin Y, Yip HK, Samaranyake YH, Yau JY, Samaranyake LP. 2003. Biofilm-forming ability of *Candida albicans* is unlikely to contribute to high levels of oral yeast carriage in cases of human immunodeficiency virus infection. J Clin Microbiol 41:2961–2967. <https://doi.org/10.1128/JCM.41.7.2961-2967.2003>.
  67. Nimrichter L, Burdick MM, Aoki K, Laroy W, Fierro MA, Hudson SA, Von Seggern CE, Cotter RJ, Bochner BS, Tiemeyer M, Konstantopoulos K, Schnaar RL. 2008. E-selectin receptors on human leukocytes. Blood 112: 3744–3752. <https://doi.org/10.1182/blood-2008-04-149641>.
  68. de Menezes-Neto A, Sáez MJF, Lozano-Ramos I, Seguí-Barber J, Martín-Jaular L, Ullate JME, Fernández-Becerra C, Borrás FE, Del Portillo HA. 2015. Size-exclusion chromatography as a stand-alone methodology identifies novel markers in mass spectrometry analyses of plasma-derived vesicles from healthy individuals. J Extracell Vesicles 4:27378. <https://doi.org/10.3402/jev.v4.27378>.
  69. Lowry RR. 1968. Ferric chloride spray detector for cholesterol and cholesteryl esters on thin-layer chromatograms. J Lipid Res 9:397. [https://doi.org/10.1016/S0022-2275\(20\)43112-8](https://doi.org/10.1016/S0022-2275(20)43112-8).
  70. Fuchs BB, Mylonakis E. 2006. Using non-mammalian hosts to study fungal virulence and host defense. Curr Opin Microbiol 9:346–351. <https://doi.org/10.1016/j.mib.2006.06.004>.